

STEADY WAVE DRIFT FORCE ON BASIC OBJECTS OF SYMMETRY

A Thesis

by

ANUPAM GUPTA

Submitted to the Office of Graduate Studies of
Texas A&M University
in partial fulfillment of the requirements for the degree of

MASTER OF SCIENCE

August 2008

Major Subject: Civil Engineering

STEADY WAVE DRIFT FORCE ON BASIC OBJECTS OF SYMMETRY

A Thesis

by

ANUPAM GUPTA

Submitted to the Office of Graduate Studies of
Texas A&M University
in partial fulfillment of the requirements for the degree of

MASTER OF SCIENCE

Approved by:

Chair of Committee,	John M. Niedzwecki
Committee Members,	H. Joseph Newton
	James Kaihatu
Head of Department,	David V. Rosowsky

August 2008

Major Subject: Civil Engineering

ABSTRACT

Steady Wave Drift Force on Basic Objects of Symmetry.

(August 2008)

Anupam Gupta, B.Tech., Banaras Hindu University

Chair of Advisory Committee: Dr. John M. Niedzwecki

An exponential growth in the offshore industry has resulted in a corresponding increase in demand for quick, accurate, and implementable designs. With the increase in size of the structure relative to the wave amplitude, analysis should be performed using the diffraction theory. The steady wave drift force on a submerged body is a second-order quantity. With a potential flow assumption, the force arises from the diffraction and radiation of the waves from the interaction with the body. For a fixed body in waves the steady force is contributed from the wave diffraction effect alone. Numerical solutions for are generally needed for the computation of the steady drift force on submerged structures. In this study the steady wave drift forces on several fixed bodies of basic shapes are derived in closed form. The thesis addresses the steady drift forces on the following basic structures: a box, a vertical circular cylinder, a submerged horizontal cylinder, a bottom-seated horizontal half cylinder, a bottom-seated hemisphere, a submerged sphere, and an ellipsoid. The results developed demonstrate the importance of various independent non-dimensional parameters.

To achieve speed and accuracy of the analytical/numerical solutions for the second

order forces on the basic bodies with symmetry has been presented. Mathematical formulation of the boundary value problem and its second order solution have been described using the different coordinates depending on the symmetry and nature of the object. Charts and formulas have been developed to provide solution for the second order wave forces on different basic structures like cylinder, sphere and ellipsoids. This study is helpful for a first pass estimate of the steady drift force where the translational and rotational contributions are neglected. The illustrative examples provide a sense of the accuracy and an approach to bound the results of complex geometries by approximating them as simpler geometries.

DEDICATION

To my parents

ACKNOWLEDGEMENTS

Partial financial support for this research from the R.P Gregory'32 Chair endowment and the Texas Engineering Experiment Station is gratefully acknowledged.

I would like to express my gratitude and thanks to my advisor, Dr. John M. Niedzwecki, for his guidance and advice during my studies. I would also like to thank Dr. S. Chakrabarti who guided me in the initial stages of research. I would also like to thank my advisory committee members: Dr. Joseph H. Newton and Dr. James Kaihatu, for their guidance throughout this research project.

TABLE OF CONTENTS

	Page
ABSTRACT	iii
DEDICATION.....	v
ACKNOWLEDGEMENTS.....	vi
LIST OF TABLES.....	ix
LIST OF FIGURES	x
1. INTRODUCTION	1
1.1 Literature Review	1
1.2 Research Objective	7
2. MATHEMATICAL FORMULATION.....	8
2.1 Surface Piercing Bodies.....	13
2.1.1 Vertical Cylinder	13
2.1.2 Rectangular Submerged Bodies	18
2.2 Bottom Mounted Submerged Bodies	22
2.2.1 Bottom Mounted Horizontal Half Cylinder	22
2.2.2 Bottom Mounted Hemisphere	27
2.3 Submerged Bodies	31
2.3.1 Horizontal Cylinder.....	31
2.3.2 Submerged Sphere.....	34
2.3.3 Submerged Ellipsoid	38
3. IMPLEMENTATION	42

	Page
4. STEADY DRIFT FORCE NUMERICAL EXAMPLES	46
4.1 Basic Body Geometries	46
4.2 Effect of Neglecting Translation and Rotation Contribution	58
4.2.1 Barge	58
4.2.2 Sphere.....	63
4.3 Approximations Using Ellipsoidal Geometries.....	66
4.3.1 Autonomous Underwater Vehicle (AUV).....	66
4.3.2 Fish.....	72
5. SUMMARY AND CONCLUSIONS.....	76
REFERENCES	78
APPENDIX 1 SYMBOLS.....	83
APPENDIX 2 MATLAB CODE.....	85
VITA.....	90

LIST OF TABLES

TABLE		Page
1	Values of Integrals $I_1'(ka)$ and $I_2'(ka, s_0/a)$	25
2	Properties for Barge Example.....	60
3	Properties for AUV Example.....	68
4	Overall Lengths of the Different Fishes (Haslett [13]).....	73

LIST OF FIGURES

FIGURE		Page
1	Definition sketch of a vertical cylinder.....	15
2	Definition sketch of a rectangular body.....	19
3	Definition sketch of a bottom mounted horizontal half cylinder.....	23
4	Definition sketch of a bottom mounted hemisphere.....	28
5	Definition sketch of a horizontal cylinder.....	32
6	Definition sketch of a sphere.....	35
7	Definition sketch of an ellipsoid	39
8	Steady drift force on a vertical cylinder.....	47
9	Steady drift force on a horizontal cylinder.....	49
10	Steady drift force on a horizontal half cylinder.....	50
11	Steady drift force on a hemisphere.....	51
12	a) Steady drift force on a sphere b) F_{max} values of sphere.....	54
13	a) Steady drift force on an ellipsoid with constant a and b b) Steady drift force on an ellipsoid with constant a and c.....	55
14	Comparison of sphere and ellipsoid results.....	57
15	a) Graph from Choi et al.[7] b) Validation of barge example with Choi et al. [7] c) Comparison of free surface and velocity squared component with total force from Choi et al. [7].....	61
16	a)Validation of sphere result with Wu et al. [39] b) Graph from Wu et al. [39] c) Ratio of velocity squared term to total force.....	64

FIGURE		Page
17	a) Description of AUV example (Wang et al.(49)) b) Different areas of cross-section c) Drift force on AUV.....	69
18	a) Geometrical approximation of different fishes b) Drift force on fishes.....	74

1. INTRODUCTION

1.1 Literature Review

With increasing utilization of coastal and ocean areas, more recent research studies have focused upon optimizing the accuracy and speed in the analysis and design of offshore structures. It is necessary in the design of these structures to evaluate wave forces acting on them as accurately as possible. The Morison equation [4] is useful in estimating the wave forces acting on cylindrical structural element or ocean platforms whose characteristic dimension is much smaller than the incident wavelength. As the size of these dimension increase and approach to the order of the wavelength, the Morison type equation becomes less accurate and the diffraction theory is needed to more accurately estimate the wave forces.

A lot of research studies have been reported in the literature that deal with first and second order diffraction and radiation theory and drift forces; see for example Garrison and Rao [12] and Chakrabarti and Naftzger [6]. Most of the studies are numerical methods and their approach takes a lot of computational effort and time. A lot less research has been directed to develop efficient approaches that combine analytical and numerical procedures for estimating the wave forces on the offshore structures, in part, because of the mathematical complexity involved in calculation of forces. Although advances in this regard are reflected in the studies reported by Kim and Yue [16] and Newman [26]. Closed form solutions can be obtained for some basic shapes, which generally reflect the shape of many offshore structures. These results can be compiled to provide a convenient solution

for the engineers to get a preliminary assessment of the second order drift forces, and this is the focus of the research study.

Faltinsen [8] in his book provides an excellent discussion of the second order nonlinear forces and their importance in several context of marine structures, and includes the design of mooring systems, thruster systems, analysis of offshore loading systems and evaluation of towing of large gravity platforms. He provides a detailed explanation of the different drift forces including both the theory and the examples which illustrate the importance of analysis of second order forces on the different bodies.

The earliest work on diffraction effect involved the solution of linear wave interaction with a vertical cylinder by MacCamy and Fuchs [20]. This was closely followed by the work of Havelock [14] who discussed the diffraction force acting on a submerged sphere under deepwater wave condition. His formulation did not consider the free surface boundary condition and consequently, the effects of the bottom boundary and free surface boundaries on the acting wave force cannot be evaluated. Garrison and Rao [12] and Chakrabarti and Naftzger [6] discussed the effect of the free surface on the acting wave force in the case of a bottom-seated hemisphere. Both research studies reported that the free surface boundary was negligible effect if the radius was less than half the water depth. In 1975 Black [2] studied the diffraction force acting on a sphere whose center was fixed at the still water level. He developed a numerical solution using an axisymmetric Green's function and concluded that the bottom boundary has little effect on the wave force when water depth is larger than twice the sphere radius. This was also confirmed in a later study by Fenton [11]. The diffraction force acting on a fully submerged sphere in finite water

depth, where the bottom and free surface boundary conditions are both included is less well studied. Mizutani and Itawa [23] investigated the diffraction force on a submerged spherical structure and wave diffraction and concluded that the diameter and submergence affect the forces, and that the wave heights have very little effect on it. Zhao et al. [40] investigated the magnitude of the mean wave forces relative to the linear first order wave forces for a hemisphere floating in the free surface. They concluded that as the wave amplitude increases the effect of the second order forces relative to the first order forces increases.

Mauro [21] developed a formula based on the momentum conservation approach to calculate the drift forces on the two dimensional body in incident regular deep water waves for a fixed or floating bodies. He assumed no current and no body speed for his calculations. This formula was later on generalized by Longuet – Higgins and Prazdny [19] for a finite water depth by introducing a multiplicative factor. Newman [25] using same method calculated drift moment and forces on a slender body. Remery and Oortmerssen [35] extended the work of Mauro by giving formulas of drift forces for tankers and semi-submersibles. Both the momentum and pressure integration approach for drift force calculations was summarized by Ogilvie [30].

Faltinsen and Michelsen [10] computed drift forces on floating structures by using the Green function approach, and showed their good agreement with the experimental data. Pinkster and Oortmerssen [32] and Pinkster [33] studied second order steady forces and low frequency second order forces using 3-D diffraction/radiation theory. Later Papanikolau and Zaraphonitis [31] derived the steady drift forces using the same technique.

Faltinsen and Loken [9] summarized the work of different researchers and produced comparison of the different model. Wu et al.[39] presented the solution for the second order drift forces using the far field and near field approach on a sphere in finite water depth. Their model only considered for the diffraction contribution to the drift force, however results obtained by them were in close agreement with the numerical solutions by Wang [38].

A formulation for second order drift forces on slow moving vehicles based on law of conservation of impulse over fluid domain was developed by Hermans and Sierrevogel [15]. Their numerical investigations led them to conclude that the small first order forces at low frequencies can generate significant high second order forces

Several two dimensional approaches has been followed in literature for calculation of drift forces using diffraction theory. These include strip theory (Mathisen et al. [22]), macro-element (Kokkinowrachos and Zibell [17]), and source and sink method (Naftzger and Chakrabarti [4]). Among all of these two strip theory method is the oldest and has been used most extensively. In developing the two strip theory Matheisen et al. [22] improved strip theory approach by considering the opposed motion potentials due to interaction of pontoons. According to this theory radiation potential and the coefficients associated with it are calculated and total force is calculated using Haskinds Relations.

Skourup et al. [36] investigated non linear loads on fixed body due to waves and current using Potential theory and 3-D Boundary Element Method (BEM) and computed

second order oscillatory and steady forces on a vertical circular cylinder using time stepping procedures. Based upon their computation they concluded that the second order amplitude and the current have significant influence on the forces. Li and Williams [18] worked on the diffraction of the second order biochromatic waves by a semi-immersed horizontal rectangular cylinder. Analytical expressions for the velocity potentials in each region for first- order and second-order contributions were obtained using an eigen function expansion approach.

Newman and Scalvounous [29], discussed a new panel program for computation of wave loads on large offshore structures using Greens identity. An integral equation was developed for the velocity potential on the body surface and was computed using the Green's function. Integral Equations were solved using WAMIT. The integral equations were also discretized in N panels and developing a system of N complex linear algebraic equations with the same number of unknowns. For the convergence of the equation the panels were spaced near to the corner which showed that that a careful discretization can lead to the reasonable levels of engineering accuracy for the structures considered with less than 100 panels. Computational results were presented for the Catamaran Barge which revealed the importance of three dimensional effects on the resonant gap motions. Authors also recommended for future work which includes the implementation of a complete second order solution, including both the sum and difference frequency forces acting on a body in a spectrum of waves. Molin et al. [24], discussed the non linear wave interaction with a square cylinder. They validated the Boussinesq's model against the WAMIT results for first order and second order. The results obtained were in fair agreement with the Boussinesq's model.

Newman and Lee [27] discussed the radiation problems with the exact geometries focusing on the use of B Splines. Instead of using explicit geometry they used the approach where B Splines are used to define geometry as well as the velocity potential. Three examples were presented of vertical cylinder, toroid and rectangular barge with moon pool. They showed that higher order solution is much more accurate and required less number of unknowns. Also when the draft in case of the barge was reduced corresponding wave number increased. Lee and Newman [28], described the development of the panel method in detail. They described the formulation of Boundary value problem, integral equation, Mean drift forces, fluid velocity leading to the panel method. They also reviewed the pFFT method and the second order forces. The use of B splines was discussed in the higher order panel method . Numerical example on FPSO showed the accuracy of second order forces. Also the pFFT method was proved to be faster but it was restricted to use with the low order panel method. Also they concluded that for the objects with planes of symmetry the computational domain may be reduced remarkably.

Bora [3] et al. presented analytical results to the wave diffraction and radiation problems using Legendre polynomial for a submerged sphere. He developed the analytical expressions for various hydrodynamic coefficients and exciting force. Velocity potential was expressed as a series of Legendre polynomial using the theory of infinite expansions. Using the analytical expressions numerical estimates for hydrodynamic coefficients and exciting forces are presented.

1.2 Research Objective

The objective of this research study is to develop a hybrid analytical and numerical procedure that allows a rapid evaluation of the second order drift forces. There are a variety of common shapes that are used in the design of offshore structures some of which can be used to approximate to more complex offshore structures. For example vertical cylindrical shape can be used to model monotower platforms or monocolumn wind turbine towers, spar platforms and similar surface piercing cylinders. Further, fully submerged ellipsoidal shapes can be used to model Autonomous Underwater Vehicles (AUVs) or even fish. Thus the second order mean drift forces on the ellipsoidal shapes can be calculated using the proposed methodology. The body shapes to be addressed include surface piercing vertical cylinder, submerged horizontal cylinder, bottom seated hemispherical and rectangular bodies and submerged spherical and ellipsoidal bodies. The wave are assumed to be regular with no current, however a study can be carried out to calculate the similar results in the current to account the forces generated due to the current.

2. MATHEMATICAL FORMULATION

A brief summary of the first and the second order potential theory is provided in order to present the second order diffraction force equation within the context of radiation/diffraction analysis. More detailed descriptions can be found for example in the book, “Hydrodynamics of Offshore Structure”, by S. K . Chakrabarti [4].

The governing equation in this study is developed assuming the fluid to be inviscid, incompressible and irrotational and consequently the fluid velocity field may be represented as the gradient of the scalar potential, for e.g. $\phi(x,y,z,t)$ for Cartesian coordinate. Other coordinate systems will be utilized such as ellipsoidal, spherical, cylindrical depending up on the application. Once the velocity potential is known the steady drift forces on the fixed body can be computed. The velocity potential is computed by developing a boundary value problem using the usual assumptions of the radiation/diffraction theory. (Chakrabarti [4]). For the convenience of the solution the ϕ is assumed to take the form of a power series with respect to a perturbation parameter. The index of the power series represents the order of the theory. First, second and higher order solutions are calculated by the researcher depending on the type of solution desired. After the estimation of ϕ , first order forces and the second order forces can be calculated.

The steady drift force due to the incident wave on any symmetric body with respect to wave direction can be shown to be identically zero due the symmetry of the pressure distribution. Thus the contribution on the second-order drift force comes from the diffraction potential.

The potential function can be expressed as the sum of scattered (ϕ_d) and incident velocity potential (ϕ_i).

$$\phi = \phi_d + \phi_i \quad (1)$$

The total potential ϕ is obtained by solving the Laplace equation, which in the Cartesian Coordinates is

$$\begin{aligned} \nabla^2 \phi(x_i, t) &= 0 \\ \frac{\partial^2 \phi}{\partial x^2} + \frac{\partial^2 \phi}{\partial y^2} + \frac{\partial^2 \phi}{\partial z^2} &= 0 \end{aligned} \quad (2)$$

where, the spatial coordinates, x, y and z represents a point in the fluid where the potential is calculated at anytime t.

The boundary conditions consist of the dynamic and kinematic boundary conditions at free surface and bottom boundary condition. At the free surface elevation, η , the total dynamic pressure is equal to the atmospheric pressure which is constant, leading to the dynamic free surface condition

$$\frac{\partial \phi}{\partial t} + g\eta + \frac{1}{2} \left(\left(\frac{\partial \phi}{\partial x} \right)^2 + \left(\frac{\partial \phi}{\partial y} \right)^2 + \left(\frac{\partial \phi}{\partial z} \right)^2 \right) = 0 \quad (3)$$

Similarly, the kinematic free surface boundary condition is given by

$$\frac{\partial \eta}{\partial t} + \frac{\partial \phi}{\partial x} \frac{\partial \eta}{\partial x} + \frac{\partial \phi}{\partial y} \frac{\partial \eta}{\partial y} + \frac{\partial \phi}{\partial z} \frac{\partial \eta}{\partial z} - \frac{\partial \phi}{\partial y} = 0 \quad (4)$$

the bottom boundary condition, can be derived based on the fact that the vertical velocity of water particle at the bottom surface is equal to zero assuming that the ocean floor is flat.

$$\frac{\partial \phi}{\partial y} = 0 \quad (5)$$

Another boundary condition can be obtained by equating the normal component of the water particle velocity to the velocity of the body, since we have assumed the zero velocity for the body, the normal component of the water particle velocity will be equal to zero, which can be expressed mathematically as

$$\frac{\partial \phi}{\partial \eta} = 0 \quad (6)$$

Introducing eq (1), the body surface condition can be rewritten as

$$\frac{\partial \phi_d}{\partial \eta} = -\frac{\partial \phi_i}{\partial \eta} \quad (7)$$

Then as one move away from the body surface a distance R_0 , the scattered potential (ϕ_s) decreases and eventually vanishes at infinity. This line of reasoning leads to the Sommerfield radiation condition,

$$\lim_{R \rightarrow \infty} \sqrt{R_0} \left(\frac{\partial}{\partial R} \pm i\zeta \right) \phi_d = 0 \quad (8)$$

Solution of this nonlinear boundary value problem is complicated, so perturbation techniques are commonly employed to obtain a solution to this problem. Accordingly, a power series is introduced of the form

$$\phi = \sum_{n=1}^N \varepsilon^n \phi_n \quad (9)$$

where, the perturbation parameter ε is equal to the product of the wave number k and the wave amplitude, a and the symbol n represents an n th order approximation. Similarly utilizing water surface elevation, η , one obtains the perturbation equation

$$\eta = \sum_{n=1}^N \varepsilon^n \eta_n \quad (10)$$

For this study, the focus will be upon the first and the second order forces and the approximation of higher order terms will be assumed to be negligible. Once the first and second order potentials are evaluated, dynamic pressure can be calculated using the Bernouli's equation which can be expressed as

$$p = \rho \frac{\partial \phi}{\partial t} + \frac{1}{2} \rho (\nabla \phi)^2 \quad (11)$$

where, ρ is density of ocean water and $\nabla \phi$ is the shorthand notation for the gradient.

On solving this boundary value problem, the velocity potential due to linear wave is obtained for a right-handed coordinate system located at the still water level which can be expressed as

$$\phi(x, y, z, t) = i \frac{gH}{2\omega} \frac{\cosh k(z+d)}{\cosh kd} \exp i [k \{x \cos \beta + y \sin \beta\} - \omega t] \quad (12)$$

where g is the gravitational acceleration, H is wave height and here it is assumed to be twice the wave amplitude, ω is the circular wave frequency, d is the water depth, k is the wave number and β is the angle of direction of wave propagation.

It can be further shown that the horizontal component of the velocity along the x direction is

$$u(x, y, z, t) = -\frac{gkH}{2\omega} \cos \beta \frac{\cosh k(z+d)}{\cosh kd} \exp i [k(x \cos \beta + y \sin \beta) - \omega t] \quad (13)$$

$$= ik\phi \cos \beta$$

and along the y direction is

$$v(x, y, z, t) = -\frac{gkH}{2\omega} \sin \beta \frac{\cosh k(z+d)}{\cosh kd} \exp i [k(x \cos \beta + y \sin \beta) - \omega t] \quad (14)$$

$$= ik\phi \sin \beta$$

Similarly, vertical velocity component along the vertical z direction is

$$w(x, y, z, t) = i \frac{gkH}{2\omega} \frac{\sinh k(z+d)}{\cosh kd} \exp i [k \{x \cos \beta + y \sin \beta\} - \omega t] \quad (15)$$

The total pressure at a certain depth is the sum of the atmospheric pressure, the hydrostatic pressure and the dynamic pressure which is given by

$$p(x, y, z, t) = \frac{\rho g H}{2\omega} \frac{\cosh k(z+d)}{\cosh kd} \exp i [k \{x \cos \beta + y \sin \beta\} - \omega t] \quad (16)$$

The second order forces are calculated using the Bernoulli equation and they have been found to have two main components (\bar{F}_j) denoted with the subscripts j (Chakrabarti and Gupta [5]). The first is mean drift force due to free surface effect, \bar{F}_1 which is obtained by integrating the free surface elevation over the wavelength. It can be expressed as

$$\bar{F}_1 = \frac{1}{2} \rho g \int_{WL} \eta_{r=a}^2 n \, dl \quad (17)$$

where $\eta_{r=a}$ wave surface elevation at the body surface, n is the surface direction normal, and WL is the waterline of the body in still water. The second contribution to the mean drift

force, \bar{F}_2 , arises from the velocity squared term in the Bernoulli's equation and can be expressed as

$$\bar{F}_2 = \frac{1}{2} \iint_{S_0} \rho \sum_{j=1}^N u_j^2 n dS \quad (18)$$

where u_j represents the water particle velocity component along the N body coordinates and dS is the elemental area on the submerged part of the body surface up to the still water level, S_0 . The third component of the drift force, due to motion term is

$$\bar{F}_3 = \rho \iint_{S_0} X' \frac{\partial \phi}{\partial t} n dS \quad (19)$$

where again the integration is elevated over the body surface and X' represents the translational body motion of inertia i.e surge, sway or heave. The fourth component of the mean drift force is due to rotation of body and can be expressed as

$$\bar{F}_4 = S \times \bar{F}_3 \quad (20)$$

where S is the radius of the gyration corresponding to the surge or sway motion of the body. For additional discussion see for example, Chakrabarti (pp 260-262) [4].

2.1 Surface Piercing Bodies

2.1.1 Vertical Cylinder

Vertical Cylinders are one of the most commonly used structural geometries found in the design of offshore structures. They may serve as the main structural components of steel caissons, wind turbine towers or jacket structures. A schematic of a vertical bottom founded cylinder is presented in Fig. 1. The origin of the cylindrical coordinate system is located at

the seabed and is aligned with the center line of the cylinder. At the outer surface of the cylindrical hull, $r = a$, the incident wave surface profile can be expressed in terms of Bessel functions of the first kind, J_n and Kronecker delta function, δ , specifically (Chakrabarti [4]).

$$\eta(r, \theta, t) = \frac{H}{2} \sum_{n=0}^{\infty} \delta_n i^{n+1} J_n(ka) \cos n\theta \exp(-i\omega t) \quad (21)$$

It follows that the mean drift force due to free surface effect can be expressed as

$$\bar{F}_1 = \frac{1}{2} \frac{\rho g a H^2}{4} \int_0^{2\pi} \left[\left\{ \sum_{n=0}^{\infty} \delta_n i^{n+1} J_n(ka) \cos n\theta \exp(-i\omega t) \right\}^2 \right] \cos \theta d\theta \quad (22)$$

However it is more convenient to introduce an alternate form of eq (22) which leads to a more compact dimensionless expression. The real part of velocity potential at the cylinder surface may be written in the terms of Fourier series expansion with coefficients, a_n and b_n , that will later be defined in terms of Bessel function

$$\phi(r = a, \theta, t) = \frac{Hg}{2\omega} \frac{2}{\pi ka} \sum_{n=0}^{\infty} \delta_n [a_n \cos \omega t + b_n \sin \omega t] \cos n\theta \quad (23)$$

At the free surface wave profile at $r=a$ can be expressed as

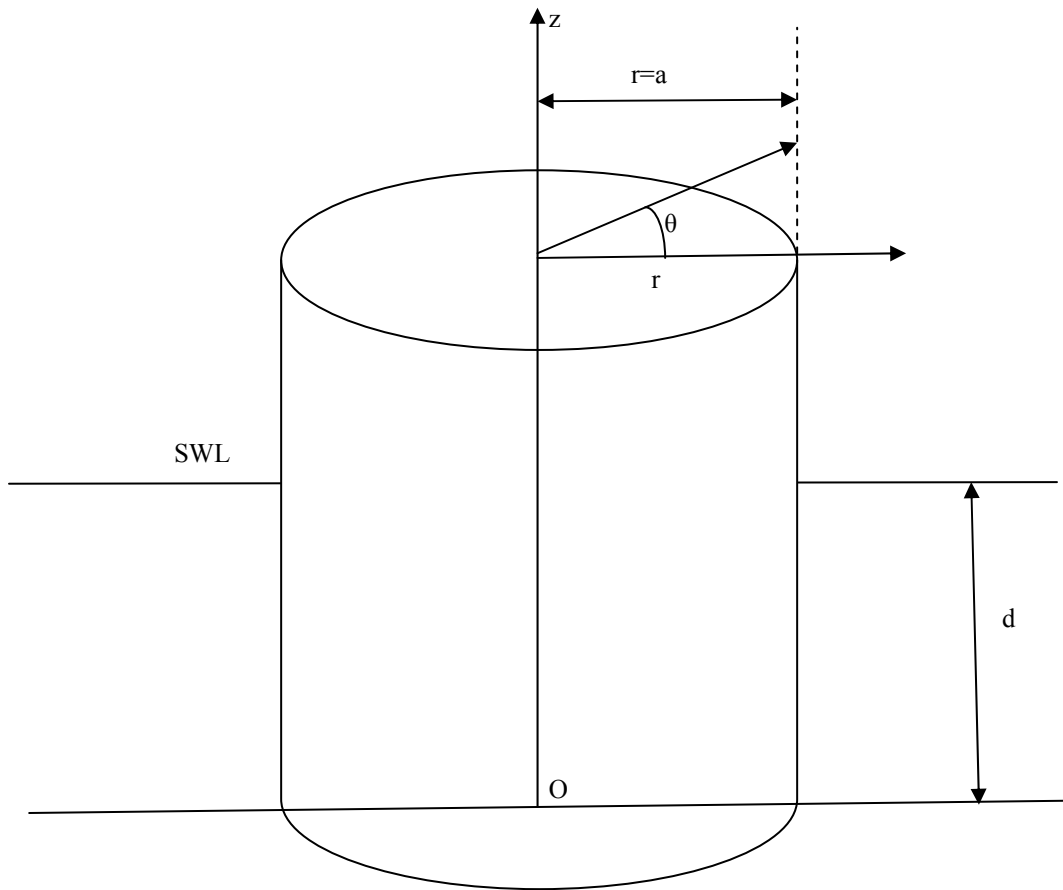


Fig.1 Definition sketch of a vertical cylinder

$$\eta(a, \theta, t) = \frac{H}{2} \frac{2}{\pi ka} \sum_{n=0}^{\infty} \delta_n [-a_n \sin \omega t + b_n \cos \omega t] \cos n\theta \quad (24)$$

Then the mean drift force due to free surface effect can now be alternatively expressed as

$$\begin{aligned} \bar{F}_1 &= \frac{1}{2} \rho g \int_{WL} \eta^2 \cos \theta dl \\ &= \frac{1}{2} \rho g \left(\frac{2}{\pi ka} \right)^2 \left(\frac{H}{2} \right)^2 \int_0^{2\pi} \sum_{n=0}^{\infty} [-\delta_n a_n \sin \omega t + \delta_n b_n \cos \omega t] \cos n\theta \\ &= \sum_{m=0}^{\infty} [-\delta_m a_m \sin \omega t + \delta_m b_m \cos \omega t] \cos m\theta \cos \theta d\theta \end{aligned} \quad (25)$$

On separating out the time independent part from the above term and then simplifying the force term, the dimensionless mean drift force term can be expressed compactly as

$$F_1 = \frac{4}{\pi (ka)^2} \sum_{n=0}^{\infty} a_n a_{n+1} + b_n b_{n+1} \quad (26)$$

where,

$$F_1 = \frac{\bar{F}_1}{\rho g \left(\frac{H}{2} \right)^2 a} \quad (27)$$

and a_i and b_i are defined as

$$\begin{aligned}
a_{2n} &= (-1)^n \frac{J'_{2n}(ka)}{A'_{2n}(ka)} \\
a_{2n+1} &= (-1)^{n+1} \frac{Y'_{2n+1}(ka)}{A'_{2n+1}(ka)} \\
b_{2n} &= -(-1)^n \frac{Y'_{2n}(ka)}{A'_{2n}(ka)} \\
b_{2n+1} &= (-1)^{n+1} \frac{J'_{2n+1}(ka)}{A'_{2n+1}(ka)} \\
A_n(ka) &= [J'_n(ka)]^2 + [Y'_n(ka)]^2
\end{aligned} \tag{28}$$

where J'_n and Y'_n are the Bessel functions (Abramowitz and Stegun [1]).

Similarly for the velocity squared term, one can obtain the corresponding mean drift force component by first differentiating the potential function and then using the formula as described by eq (18) one can obtain the normalized drift force as follows

$$\overline{F_2} = \frac{\rho}{2} \iint_S (u_\theta^2 + u_r^2) dS \tag{29}$$

where,

$$\begin{aligned}
u_\theta &= \frac{\partial \phi}{\partial \theta} \\
u_r &= \frac{\partial \phi}{\partial r}
\end{aligned} \tag{30}$$

$$\overline{F_2} = \frac{2\rho g(H/2)^2 a}{\pi(ka)^2} \left\{ \left[1 - \frac{2kd}{\sinh 2kd} \right] \sum_{n=0}^{\infty} a_n a_{n+1} + b_n b_{n+1} \right. \\
\left. + \left[1 + \frac{2kd}{\sinh 2kd} \right] \frac{\sum_{n=0}^{\infty} (a_n a_{n+1} + b_n b_{n+1}) n(n+1)}{(ka)^2} \right\} \tag{31}$$

$$F_2 = \frac{\overline{F_2}}{\rho g (H/2)^2 a} = \frac{2}{\pi (ka)^2} \left\{ \left[1 - \frac{2kd}{\sinh 2kd} \right] \sum_{n=0}^{\infty} a_n a_{n+1} + b_n b_{n+1} \right. \\ \left. + \left[1 + \frac{2kd}{\sinh 2kd} \right] \frac{\sum_{n=0}^{\infty} (a_n a_{n+1} + b_n b_{n+1}) n(n+1)}{(ka)^2} \right\} \quad (32)$$

Since there is no translation and rotational motion $F_3 = F_4 = 0$.

2.1.2 Rectangular Submerged Bodies

Consider a rectangular box located in water depth d , submerged in the water depth D . The box has length l , a width b , a height h and origin to the coordinate system is located at depth D below still water level as shown in Fig. 2. It has been assumed that the depth of submergence D is smaller than the height h to include the free surface effect. Also assume that the wave is traveling from $-x$ to $+x$ so that $\beta = 0$ and the potential function can be expressed as

$$\phi(x, y, z, t) = \rho g \frac{H}{2\omega} \frac{\cosh k(z+d)}{\cosh kd} \exp i[kx - \omega t] \quad (33)$$

and the wave profile on the front and back faces of the rectangular box at the SWL is

$$\eta(t) = \frac{H}{2} \exp \left[\pm i \left(\frac{kl}{2} - \omega t \right) \right] \quad (34)$$

Thus the mean drift force due to free surface effect, taking due account of the sign of direction cosine of n_x on the two faces of the box, is given by

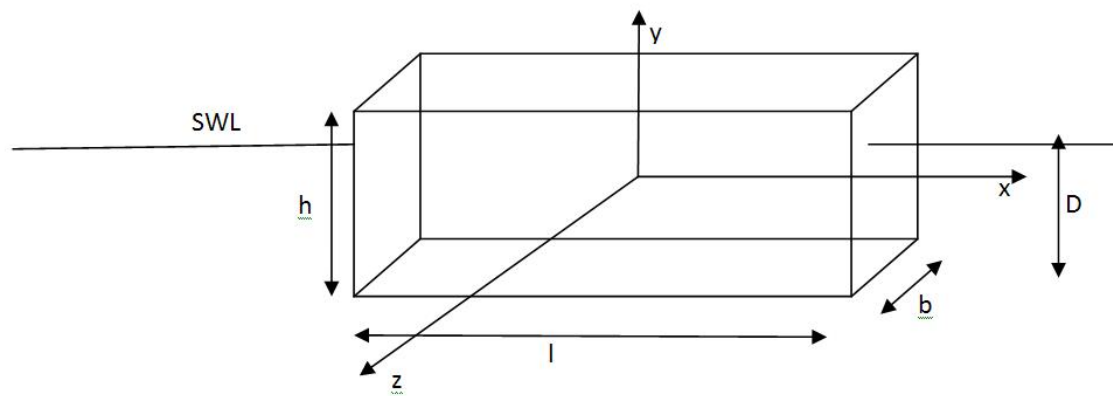


Fig. 2. Definition sketch of a rectangular body

$$\overline{F}_1 = \frac{1}{2} \rho g \int_{WL} \eta_r^2 n \, dl = \frac{1}{2} \rho g b \left[\left\{ \frac{H}{2} \exp\left(i\left(\frac{kl}{2} - \omega t\right)\right) \right\}^2 - \left\{ \frac{H}{2} \exp\left(i\left(-\frac{kl}{2} - \omega t\right)\right) \right\}^2 \right]$$

$$\overline{F}_1 = \frac{H^2}{8} \rho g b \left[\left\{ \exp\left(i\left(\frac{kl}{2} - \omega t\right)\right) \right\}^2 - \left\{ \exp\left(-i\left(\frac{kl}{2} + \omega t\right)\right) \right\}^2 \right] \quad (35)$$

$$\overline{F}_1 = \frac{H^2}{8} \rho g b \left[\left\{ \cos^2\left(\frac{kl}{2} - \omega t\right) - \sin^2\left(\frac{kl}{2} - \omega t\right) + 2i \sin\left(\frac{kl}{2} - \omega t\right) \cos\left(\frac{kl}{2} - \omega t\right) \right\} - \left\{ \cos^2\left(\frac{kl}{2} + \omega t\right) - \sin^2\left(\frac{kl}{2} + \omega t\right) - 2i \sin\left(\frac{kl}{2} + \omega t\right) \cos\left(\frac{kl}{2} + \omega t\right) \right\} \right]$$

On simplifying the above equation and integrating real part of the force term over the whole domain the value of force comes out to be:

$$\overline{F}_1 = \frac{H^2}{8} \rho g b \{ 2 \sin kl \sin(2\omega t) \} \quad (36)$$

which on averaging over one complete cycle one finds that

$$\overline{F}_1 = 0 \quad (37)$$

On differentiating the potential function with respect to the x, y and z one can obtain the water particle velocities in the respective direction. It should be noted that the velocity component along the y direction, u, is zero. The velocity squared components on a rectangular block on its front and back faces are given by

$$u^2(x, y, z; t) + w^2(x, y, z; t) = \left(\frac{gkH}{2\omega \cosh kd} \right)^2 \left[\begin{array}{l} \cosh^2 k(z+d) \cos^2 \left(\pm k \frac{l}{2} - \omega t \right) + \\ \sinh^2 k(z+d) \sin^2 \left(\pm k \frac{l}{2} - \omega t \right) \end{array} \right] \quad (38)$$

Upon carrying out the integration of the velocity squared terms from the bottom (-D) of the block to the still water level, and separating time independent term with the use of the linear wave dispersion equation

$$\omega^2 = gk \tanh 2kd \quad (39)$$

one obtains

$$\overline{F_2} = \frac{\rho g b}{4} \frac{H^2}{4} \frac{\{\sinh 2kd - \sinh 2k(d-D)\}}{\sinh 2kd} \quad (40)$$

The nondimensional form is then

$$F_2 = \frac{\{\sinh 2kd - \sinh 2k(d-D)\}}{2 \sinh 2kd} \quad (41)$$

In deep water the force term reduces to

$$F_2 = \frac{[1 - \{\cosh 2kD - \sinh 2kD\}]}{2} \quad (42)$$

Since we have assumed that there is no translation or rotational motion so $\overline{F_3} = \overline{F_4} = 0$. So

only velocity squared term contributes to the second order mean drift force.

2.2 Bottom Mounted Submerged Bodies

2.2.1 Bottom Mounted Horizontal Half Cylinder

Let us consider a horizontal half-cylinder seated on the ocean bottom of radius a and length L in a water depth d . A possible application of this geometry is the buried ocean floor pipelines used for the transportation of crude oil from the production platform to shuttle tankers or shore. Again utilizing the cylindrical coordinate system with origin located at the center of the cylinder at the seabed, as shown in the definition sketch (Fig. 3) drift forces on the half cylinder are calculated.

Based on the linear diffraction theory the dynamic pressure at the surface of the cylinder, $r = a$, has the form,

$$\phi(r, \theta; t) = \frac{gH}{2\omega} \frac{1}{\cosh kd} \sum_{n=0}^{\infty} \left[\frac{2(ika)^n}{n!} \cos n\theta \right] \exp(-i\omega t) \quad (43)$$

which can be further simplified to a more compact form given as

$$\phi(r, \theta; t) = \lambda [2 \cosh(ka \sin \theta) \exp(ika \cos \theta) - 1] \exp(-i\omega t) \quad (44)$$

Since the structure has no interaction with the surface wave, the free surface component of the drift force, F_1 , can be neglected.

The radial, r , component of velocity is zero at $r=a$. The angular, θ , component of velocity can be expressed as

$$u_{\theta}(a, \theta; t) = \lambda k \left[\begin{array}{l} \cos \theta \sinh(ka \sin \theta) \cos(ka \cos \theta) - \\ i \sin \theta \cosh(ka \sin \theta) \sin(ka \cos \theta) \end{array} \right] \exp(-i\omega t) \quad (45)$$

Since the normal velocity on the cylinder surface is zero, the only contribution to the velocity squared term on the 2-D half cylinder is

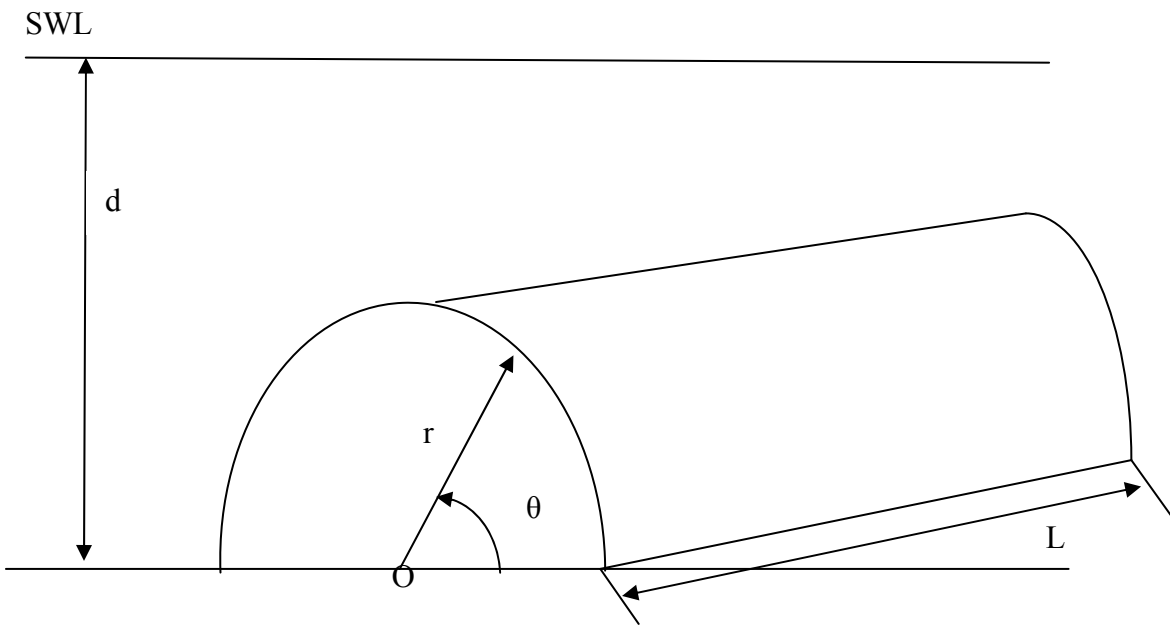


Fig. 3 Definition sketch of a bottom mounted horizontal half cylinder

$$p = \frac{1}{2} \rho u_\theta^2 = \frac{1}{2} \rho \frac{1}{r^2} \frac{\partial \phi}{\partial \theta} \quad (46)$$

$$p = \frac{1}{2} \rho u_\theta^2 = (\lambda k)^2 \left[\begin{array}{l} \cos^2 \theta \sinh^2(ka \sin \theta) \cos^2(ka \cos \theta) + \\ \sin^2 \theta \cosh^2(ka \sin \theta) \sin^2(ka \cos \theta) \end{array} \right] \quad (47)$$

Due to the symmetry of the cylindrical cross-section, horizontal surge drift force due to free surface effect and velocity-squared pressures are identically zero.

$$\overline{F_{2x}} = \frac{1}{2} \rho L \int_0^\pi u_\theta^2 \cos \theta (a d \theta) = 0 \quad (48)$$

The vertical component of the drift force is given by

$$\overline{F_{2y}} = \frac{1}{2} \rho L \int_0^\pi u_\theta^2 \sin \theta (a d \theta) \quad (49)$$

where, L is the length of the half cylinder

$$F_{2y} = \frac{\overline{F_{2y}}}{\rho g L \left(\frac{H}{2} \right)^2} = \left(\frac{2ka}{\sinh 2kd} \right) \int_0^\pi \left[\sinh^2(ka \sin \theta) - \cos^2 \theta \right] \sin \theta d\theta \quad (50)$$

which reduces to

$$F_{2y} = \left(\frac{2}{\sinh 2kd} \right) \left[I(ka) + \frac{ka}{3} \right]; \quad I(ka) = \int_0^\pi \cosh(2ka \sin \theta) \sin \theta d\theta \quad (51)$$

where, values of $I'(ka)$ can be interpolated using Table 1 where values for $I'(ka)$ are generated using the MATLAB code. Due to assumption of no translation and rotation motion, the translation and rotational component are identically zero i.e. $F_3 = F_4 = 0$.

Table 1 Values of Integrals $I_1'(ka)$ and $I_2'(ka, s_0/a)$

ka	$I_1'(ka)$	$I_2'(ka, s_0/a)$	$I_2'(ka, s_0/a)$	$I_2'(ka, s_0/a)$	$I_2'(ka, s_0/a)$
		s/a=1	s/a=1.5	s/a=2	s/a=2.5
0.1	2.0267	0.021637	0.032725	0.044142	0.056
0.2	2.1078	0.058073	0.090012	0.12556	0.16615
0.3	2.2458	0.075159	0.12118	0.1782	0.25137
0.4	2.4452	0.070808	0.12035	0.1894	0.28917
0.5	2.7124	0.056239	0.1019	0.17356	0.28953
0.6	3.056	0.040324	0.078597	0.14602	0.26762
0.7	3.4872	0.02707	0.057172	0.11645	0.23516
0.8	4.0201	0.017382	0.039996	0.089602	0.19968
0.9	4.672	0.010818	0.027232	0.067232	0.16547
1	5.4644	0.0065826	0.018182	0.04953	0.13468
1.1	6.4233	0.0039392	0.011965	0.035988	0.10813
1.2	7.5807	0.0023278	0.0077869	0.025871	0.0859
1.3	8.975	0.0013623	0.0050243	0.018443	0.067674
1.4	10.653	0.0007912	0.0032196	0.013059	0.052958
1.5	12.671	0.00045673	0.0020517	0.0091964	0.041215
1.6	15.097	0.00026236	0.0013015	0.0064469	0.031932
1.7	18.013	0.00015009	0.00082249	0.0045024	0.024646
1.8	21.519	8.5578e-05	0.00051809	0.0031343	0.018962
1.9	25.735	4.8654e-05	0.00032545	0.002176	0.014548

Table 1 continued

ka	$\Gamma_1(\mathbf{ka})$	$\Gamma_2(\mathbf{ka}, s_0/a)$	$\Gamma_2(\mathbf{ka}, s_0/a)$	$\Gamma_2(\mathbf{ka}, s_0/a)$	$\Gamma_2(\mathbf{ka}, s_0/a)$
2	30.806	2.7594e-05	0.00020396	0.0015071	0.011136
2.1	36.906	1.5616e005	0.00012755	0.0010416	0.0085061
2.2	44.248	8.8215e-06	7.9626e-05	0.00071863	0.0064856
2.3	53.085	4.9751e-06	4.9627e-05	0.00049499	0.0049371
2.4	63.726	2.8017e-06	3.0886e-05	0.00034046	0.003753
2.5	76.544	1.5757e-06	1.9197e-05	0.00023387	0.0028491
2.6	91.989	8.8519e-07	1.1918e-05	0.00016046	0.0021605
2.7	110.61	4.9674e-07	7.3914e-06	0.00010998	0.0016365
2.8	133.05	2.7848e-07	4.5796e-06	7.531e-05	0.0012384
2.9	160.12	1.5599e-07	2.8349e-06	5.1522e-05	0.00093637
3	192.77	8.7301e-08	1.7535e-06	3.522e-05	0.00070741

2.2.2 Bottom Mounted Hemisphere

Consider a hemisphere mounted at the sea bed of radius a in water depth d as shown in Fig. 4. Here we can utilize the spherical coordinates with origin at the center of the sphere at the sea bed. Based on the linear diffraction theory for a bottom-seated hemisphere the velocity potential at the surface of the cylinder, $r = a$, can be expressed in a closed form as long as the hemisphere is removed from the free surface with a d/a ratio of at least 1.5, so that its effects on the velocity potential can be ignored. In this case the expression for the velocity potential becomes:

$$\phi(r, \theta; t) = i \frac{gH}{2\omega} \frac{1}{\cosh kd} \left[\begin{array}{l} \cosh\left(\frac{r}{a} Y\right) \exp\left(i \frac{r}{a} X\right) + \\ \left[\frac{a}{r} + \frac{iX}{R^2} \right] \cosh\left(\frac{a}{r} Y\right) \exp\left(i \frac{a}{r} X\right) \\ - \frac{Y}{R^2} \sinh\left(\frac{a}{r} Y\right) \exp\left(i \frac{a}{r} X\right) - \frac{iX}{R^2} \end{array} \right] \exp(-i\omega t) a \quad (52)$$

where,

$$X = ka \cos \theta \sin \mu \quad Y = ka \sin \theta \sin \mu \quad R = ka \sin \mu \quad (53)$$

After simplifying one can obtain the time independent term for the potential function by separating the real part which can be expressed as

$$\text{Re } \phi(r, \theta; t) = \lambda \left[\begin{array}{l} - \left(2 \cosh Y - \frac{Y}{R^2} \sinh Y \right) \sin(X - \omega t) \\ - \frac{X}{R^2} \cosh Y \exp(iX) + \frac{X}{R^2} \end{array} \right] \quad (54)$$

where,

$$\lambda = gH / (2\omega \cosh kd)$$

Since the hemisphere is not having any interaction with the surface wave, the free surface term can be neglected in calculation of the drift forces

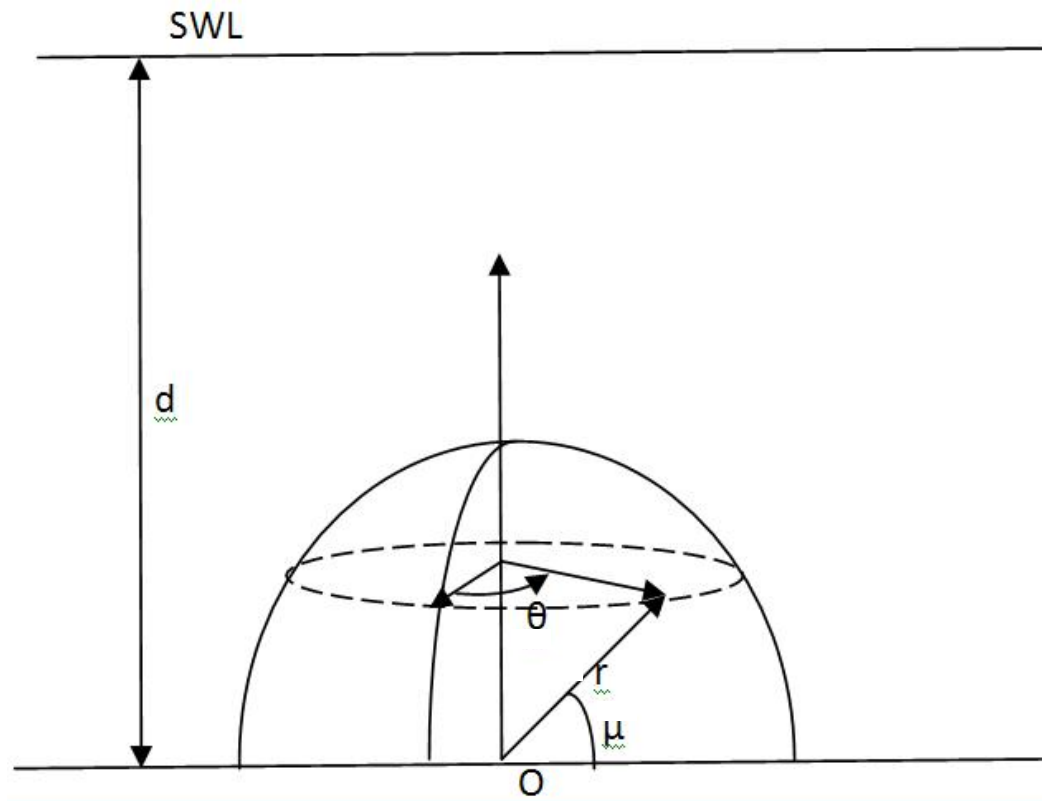


Fig.4 Definition sketch of a bottom mounted hemisphere

The angular, θ , component of the velocity can be expressed as

$$u_{\theta}(r, \theta, \mu) = \frac{1}{a \sin \mu} \frac{\partial \phi}{\partial \theta} = \frac{\lambda}{a \sin \mu} \left\{ \begin{array}{l} (2X - 2R + \frac{X}{R^2}) \sinh Y \cos(X - \omega t) + \\ \left[2Y - \frac{Y}{R^2} \right] \cosh Y \sin(X - \omega t) - \frac{Y}{R^2} \sin \omega t \end{array} \right\} \quad (55)$$

Similarly, μ , the angular component of the velocity can be expressed as

$$u_{\mu}(r, \theta, \mu) = \frac{\cot \mu}{a} \frac{\partial \phi}{\partial \mu} = \frac{\lambda \cot \mu}{a} \left\{ \begin{array}{l} -(2X - 2R + \frac{X}{R^2}) \cosh Y \sin(X - \omega t) + \\ \left[2Y - \frac{Y}{R^2} \right] \sinh Y \cos(X - \omega t) - \frac{X}{R^2} \sin \omega t \end{array} \right\} \quad (56)$$

The vertical component of velocity squared component of the steady drift force is computed from as follows

$$\overline{F_{2y}} = -\frac{1}{2} \rho a^2 \int_0^{\pi} \left(\int_0^{\pi} (u_{\theta}^2 + u_{\mu}^2) \cos \theta d\theta \right) \sin^2 \mu d\mu \quad (57)$$

And the horizontal component is given by

$$\overline{F_{2x}} = -\frac{1}{2} \rho a^2 \int_0^{\pi} \left(\int_0^{\pi} (u_{\theta}^2 + u_{\mu}^2) \sin \theta d\theta \right) \sin^2 \mu d\mu \quad (58)$$

which on substituting the velocities the and simplifying the dimensionless expression for the total force can be calculated as the follows

$$\frac{\overline{F}_2}{\rho g (H/2)^2 a} = - \left(\frac{1}{4ka \sinh 2kd} \right) \int_0^\pi \int_0^\pi \left(\begin{array}{l} \left\{ \begin{array}{l} (2X - 2R + \frac{X}{R^2})^2 \sinh^2 Y \\ + \left[2Y - \frac{Y}{R^2} \right]^2 \cosh^2 Y \\ + \left(\frac{Y}{R^2} \right)^2 \\ - 2 \frac{Y}{R^2} (2X \\ - 2R + \frac{X}{R^2}) \sinh Y \sin X \\ + 2 \frac{Y}{R^2} \left[\begin{array}{l} 2Y \\ - \frac{Y}{R^2} \end{array} \right]^2 \cosh Y \cos X \end{array} \right\} + \\ \left\{ \begin{array}{l} (2X - 2R + \frac{X}{R^2})^2 \cosh^2 Y \\ + \left[2Y - \frac{Y}{R^2} \right]^2 \sinh^2 Y \\ + \left(\frac{X}{R^2} \right)^2 \\ - 2 \frac{X}{R^2} (2X - \\ 2R + \frac{X}{R^2}) \cosh Y \cos X \\ + 2 \frac{X}{R^2} \left[\begin{array}{l} 2Y \\ - \frac{Y}{R^2} \end{array} \right]^2 \sinh Y \sin X \end{array} \right\} \cos^2 \mu \end{array} \right) \sin \theta d\theta d\mu$$

(59)

Due to assumption of no translation and rotation motion, the translation and rotational component are identically zero i.e. $F_3 = F_4 = 0$.

2.3 Submerged Bodies

2.3.1 Horizontal Cylinder

Consider the rigid horizontal cylinder of radius, $r=a$, depicted in Fig. 5. The cylinder is located at a submergence depth of s_0 in a water depth of d . Further assuming that the cylinder is rigidly constrained at elevation $d-s_0$, the incident velocity potential in the cylinder coordinate can be expressed as

$$\phi(r, \theta; t) = i \frac{gH}{2\omega} \frac{\cosh(kr \sin \theta + s_0)}{\cosh kd} \exp(ikr \cos \theta - i\omega t) \quad (60)$$

The radial, r , component of velocity on the surface of the cylinder is,

$$u_r(r = a, \theta; t) = i\lambda \left[\begin{array}{l} k \sin \theta \sinh(ka \sin \theta + s_0) + \\ ik \cos \theta \cosh(ka \sin \theta + s_0) \end{array} \right] \exp(ika \cos \theta - i\omega t) \quad (61)$$

where,

$$\lambda = \frac{gH}{2\omega \cosh(kd)}$$

The corresponding angular, θ , component of the velocity on the surface of the cylinder is

$$u_\theta(r = a, \theta; t) = i\lambda \left[\begin{array}{l} ka \sin \theta \sinh(ka \sin \theta + s_0) - \\ ika \sin \theta \cosh(ka \sin \theta + s_0) \end{array} \right] \exp(ika \cos \theta - i\omega t) \quad (62)$$

In the cylindrical coordinates the velocity-squared term on the surface of the cylinder can be expressed as

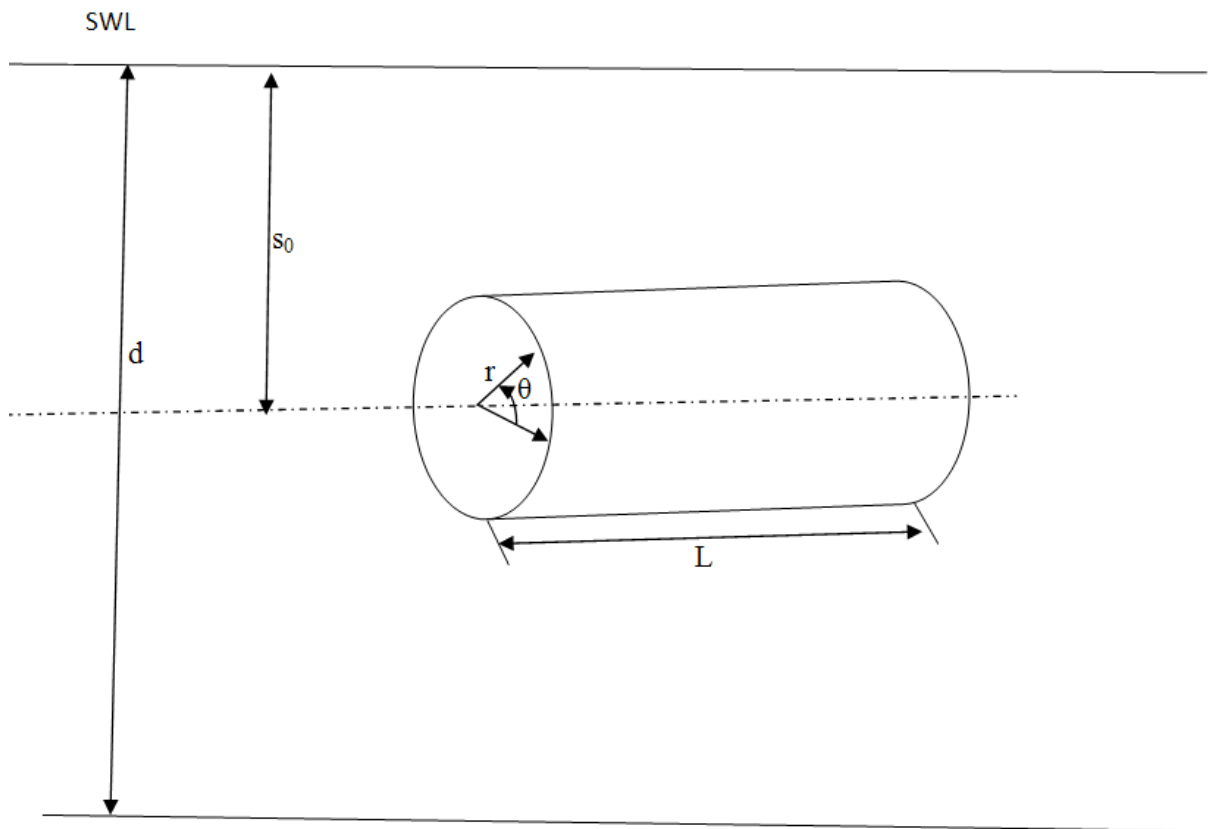


Fig.5 Definition sketch of a horizontal cylinder

$$u_{\theta}^2 + \frac{1}{r^2}u_r^2 = (k\lambda)^2 \left[\frac{(1 + \sin^2 \theta) \sinh^2(ka \sin \theta + s_0) -}{\cosh^2(ka \sin \theta + s_0)} \right] \exp 2(ika \cos \theta - i\omega t) \quad (63)$$

and the time independent velocity-squared pressure then has the form

$$u_{\theta}^2 + \frac{1}{r^2}u_r^2 = \frac{g}{a} \left(\frac{H}{2} \right)^2 \left(\frac{4ka}{\sinh 2kd} \right) \left[\frac{\cos^2 \theta \sinh^2(ka \sin \theta + ks_0) \cos^2(kas \cos \theta) +}{\sin^2 \theta \cosh(ka \sin \theta + ks_0) \sin^2(kas \cos \theta)} \right] \quad (64)$$

Due to the symmetry at the cylindrical cross-section, the horizontal component of the force is identically zero. The vertical component is obtained by evaluating the following integral

$$\overline{F}_{2y} = \frac{1}{2} \rho L \int_0^{\pi} \left(u_{\theta}^2 + \frac{1}{r^2}u_r^2 \right) \sin \theta (ad\theta) \quad (65)$$

where L is the length of the cylinder, then introducing eq (36) and eq (37) using a slightly different scaling one obtains the following dimensionless expression

$$\frac{\overline{F}_{2y}}{\rho g l \left(\frac{H}{2} \right)^2} = \left(\frac{2ka}{\sinh 2kd} \right) \int_0^{\pi} \left[\frac{\cos^2 \theta \sinh^2(ka \sin \theta + ks_0) \cos^2(kas \cos \theta) +}{\sin^2 \theta \cosh(ka \sin \theta + ks_0) \sin^2(kas \cos \theta)} \right] \sin \theta d\theta \quad (66)$$

which can be further reduced to following compact form

$$F_2 = \left(\frac{2}{\tanh kd} \right) \left[I'(ka, s_0 / r) + \frac{ka}{3} \right] \quad (67)$$

$$I'(ka, s_0 / r) = \int_0^{\pi} \cosh(2ka(\sin x + s_0 / r)) \sin x dx$$

where values of $I'(ka)$ can be obtained from Table 1 which is generated using the code for different values of ka and ratio of depth of submergence to the radius. For different values of ka or ratio of submergence depth to radius can be obtained by interpolating between the

rows or columns accordingly. Due to assumption of no translation and rotation motion, the translation and rotational component are identically zero i.e. $F_3 = F_4 = 0$.

2.3.2 Submerged Sphere

Consider a submerged sphere of radius a in a sea of water depth d in submerged at a depth of s_0 . Again we can utilize the spherical coordinates with origin at the center of sphere and at a depth of s_0 below still water level as shown in the definition sketch (Fig. 6). The potential in the spherical coordinates can be expressed as:

$$\phi(r, \theta, \mu; t) = i \frac{gH}{2\omega} \frac{1}{\cosh kd} \left[\begin{array}{l} \cosh\left(\frac{r}{a} Y\right) \exp\left(i \frac{r}{a} X\right) + \\ \left[\frac{a}{r} + \frac{iX}{R^2} \right] \cosh\left(\frac{a}{r} Y\right) \exp\left(i \frac{a}{r} X\right) \\ - \frac{Y}{R^2} \sinh\left(\frac{a}{r} Y\right) \exp\left(i \frac{a}{r} X\right) - \frac{iX}{R^2} \end{array} \right] \exp(-i\omega t) a \quad (68)$$

where, X, Y and R can be expressed as

$$X = ka \cos \theta \sin \mu \quad Y = ks_0 + ka \sin \theta \sin \mu \quad R = \sqrt{X^2 + Y^2} \quad (69)$$

The operation similar to the case of the hemisphere was performed here to simplify the potential function further as

$$\phi(r, \theta, \mu; t) = i\lambda \left[\begin{array}{l} \cosh Y \exp(iX) + \left[1 + \frac{iX}{R^2} \right] \cosh Y \exp(iX) \\ - \frac{Y}{R^2} \sinh Y \exp(iX) - \frac{iX}{R^2} \end{array} \right] \exp(-i\omega t) \quad (70)$$

where λ is defined earlier in the derivation of force for the horizontal cylinder.

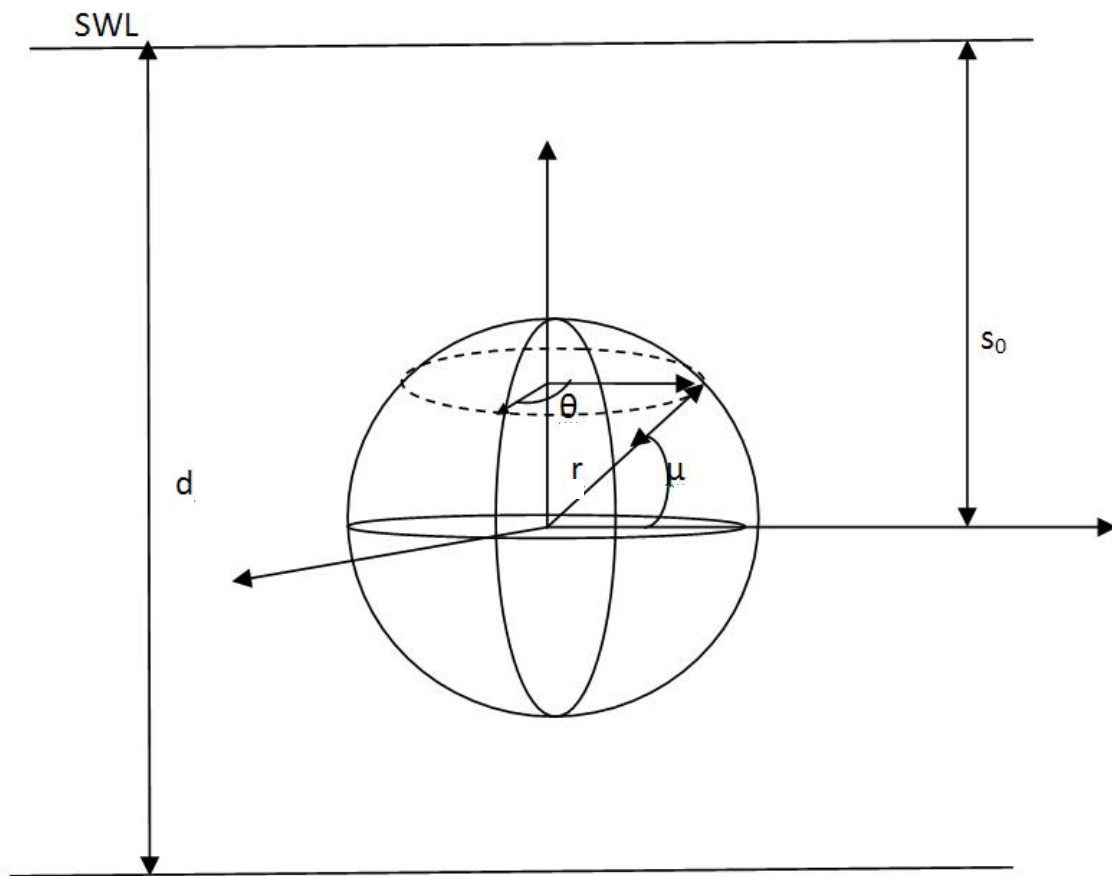


Fig.6 Definition sketch of a sphere

The time independent real part of the potential function can be obtained from the complex form by separating the real and imaginary form, which can be further used for the formulation of the forces, can be expressed as

$$\phi = \lambda \left[\begin{array}{l} -\left(2 \cosh Y - \frac{Y}{R^2} \sinh Y \right) \sin(X - \omega t) \\ -\frac{X}{R^2} \cosh Y \exp(iX) + \frac{X}{R^2} \end{array} \right] \quad (71)$$

The angular or θ , component of the velocity can be obtained from the potential as

$$u_{\theta}(r, \theta, \mu) = \frac{1}{a \sin \mu} \frac{\partial \phi}{\partial \theta} = \frac{\lambda}{a \sin \mu} \left\{ \begin{array}{l} \left(2X - 2R + \frac{X}{R^2} \right) \sinh Y \cos(X - \omega t) + \\ \left[2Y - \frac{Y}{R^2} \right] \cosh Y \sin(X - \omega t) - \frac{Y}{R^2} \sin \omega t \end{array} \right\} \quad (72)$$

Similarly the μ component of the velocity can be expressed as

$$u_{\mu}(r, \theta, \mu) = \frac{\cot \mu}{a} \frac{\partial \phi}{\partial \mu} = \frac{\lambda \cot \mu}{a} \left\{ \begin{array}{l} -\left(2X - 2R + \frac{X}{R^2} \right) \cosh Y \sin(X - \omega t) + \\ \left[2Y - \frac{Y}{R^2} \right] \sinh Y \cos(X - \omega t) - \frac{X}{R^2} \sin \omega t \end{array} \right\} \quad (73)$$

Now, since the sphere has no interaction with the surface waves only the contribution from velocity squared component of the drift force adds toward total force. The force can be calculated using the following expressions

$$\overline{F_{2x}} = -\frac{1}{2} \rho a^2 \int_0^{\pi} \left(\int_0^{2\pi} (u_{\theta}^2 + u_{\mu}^2) \cos \theta d\theta \right) \sin^2 \mu d\mu \quad (74)$$

$$\overline{F_{2y}} = -\frac{1}{2} \rho a^2 \int_0^{\pi} \left(\int_0^{2\pi} (u_{\theta}^2 + u_{\mu}^2) \sin \theta d\theta \right) \sin^2 \mu d\mu \quad (75)$$

$$\frac{\bar{F}_2}{\rho g (H/2)^2 a} = - \left(\frac{1}{4ka \sinh 2kd} \right) \int_0^\pi \int_0^{2\pi} \left(\left\{ \begin{array}{l} (2X - 2R + \frac{X}{R^2})^2 \sinh^2 Y \\ + \left[2Y - \frac{Y}{R^2} \right]^2 \cosh^2 Y + \left(\frac{Y}{R^2} \right)^2 \\ - 2 \frac{Y}{R^2} (2X - 2R + \frac{X}{R^2}) \sinh Y \sin X \\ + 2 \frac{Y}{R^2} \left[2Y - \frac{Y}{R^2} \right]^2 \cosh Y \cos X \end{array} \right\} + \left\{ \begin{array}{l} (2X - 2R + \frac{X}{R^2})^2 \cosh^2 Y \\ + \left[2Y - \frac{Y}{R^2} \right]^2 \sinh^2 Y + \left(\frac{X}{R^2} \right)^2 \\ - 2 \frac{X}{R^2} (2X - 2R + \frac{X}{R^2}) \cosh Y \cos X \\ + 2 \frac{X}{R^2} \left[2Y - \frac{Y}{R^2} \right]^2 \sinh Y \sin X \end{array} \right\} \cos^2 \mu \right) \sin \theta d\theta d\mu \quad (76)$$

Due to assumption of no translation and rotation motion, the translation and rotational component are identically zero i.e. $F_3 = F_4 = 0$.

2.3.3 Submerged Ellipsoid

Consider an ellipsoid of the major axis equal to a and the other axis as b and c ($a > b > c$), submerged in sea of water depth d at depth of s_0 . Here we can utilize the ellipsoidal coordinates $(\lambda_1, \lambda_2, \lambda_3)$ with origin at the center of the sphere at a depth of s_0 below still water level in the direction of the vertical axis as described in the definition sketch (Fig. 7). To calculate the expression for the velocity in the ellipsoidal coordinates, potential function in Cartesian coordinates was used which was then differentiated in terms of ellipsoidal coordinates using the chain rule. The potential function used can be expressed in terms of the rectangular coordinates (x, y, z) can be expressed as

$$\phi(x, y, z, t) = i \frac{gH}{2\omega} \frac{\cosh k(z+d)}{\cosh kd} \exp i [k \{x \cos \beta + y \sin \beta\} - \omega t] \quad (77)$$

Assuming that the wave is travelling along the x -axis so that the direction of the wave propagation is equal to zero ($\beta=0$), the velocity potential can be simplified to the following form

$$\phi(x, y, z, t) = i \frac{gH}{2\omega} \frac{\cosh k(z+d)}{\cosh kd} \exp i [kx - \omega t] \quad (78)$$

Now to transfer the coordinates from the rectangular to the ellipsoidal coordinates following transformation equations were used (Punzo et al.[34]).

$$\begin{aligned} x^2 &= \frac{\lambda_1^2 \lambda_2^2 \lambda_3^2}{K^2 h^2} \\ y^2 &= \frac{(\lambda_1^2 - h^2)(\lambda_3^2 - h^2)(h^2 - \lambda_2^2)}{h^2(K^2 - h^2)} \\ z^2 &= \frac{(\lambda_1^2 - k^2)(\lambda_2^2 - K^2)(K^2 - \lambda_3^2)}{k^2(h^2 - K^2)} \end{aligned} \quad (79)$$

where, K and h are defined as follows

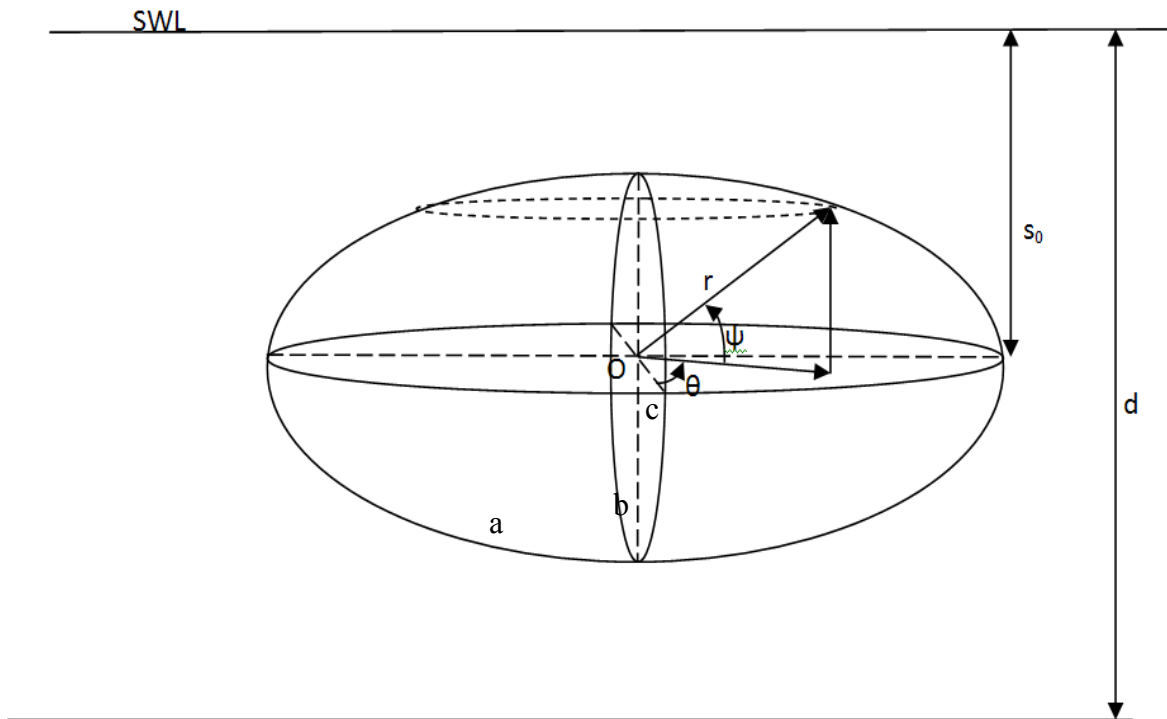


Fig.7 Definition sketch of an ellipsoid

$$\begin{aligned} K &= \sqrt{(a^2 - c^2)} \\ h &= \sqrt{(a^2 - b^2)} \end{aligned} \quad (80)$$

Using the chain rule of the differentiation and with further simplification the λ_1 component of the velocity along the major axis, u_1 can be expressed in a compact and dimensionless form as

$$\begin{aligned} u_1 &= \frac{\partial \phi}{\partial x} \frac{\partial x}{\partial \lambda_1} + \frac{\partial \phi}{\partial y} \frac{\partial y}{\partial \lambda_1} + \frac{\partial \phi}{\partial z} \frac{\partial z}{\partial \lambda_1} \\ &= \frac{2\lambda_1(\lambda_2^2 - K^2)(K^2 - \lambda_3^2)}{K^2(h^2 - K^2)z} \cdot \frac{\sinh k(s_0 + d)}{\cosh kd} \end{aligned} \quad (81)$$

velocity component along the semi major axis or λ_2 component of the velocity

$$\begin{aligned} u_2 &= \frac{\partial \phi}{\partial x} \frac{\partial x}{\partial \lambda_2} + \frac{\partial \phi}{\partial y} \frac{\partial y}{\partial \lambda_2} + \frac{\partial \phi}{\partial z} \frac{\partial z}{\partial \lambda_2} \\ &= \frac{2\lambda_2(\lambda_1^2 - K^2)(K^2 - \lambda_3^2)}{K^2(h^2 - K^2)z} \cdot \frac{\sinh k(s_0 + d)}{\cosh kd} \end{aligned} \quad (82)$$

Similarly, velocity component along the other minor axis or λ_3 component of the velocity

$$\begin{aligned} u_3 &= \frac{\partial \phi}{\partial x} \frac{\partial x}{\partial \lambda_1} + \frac{\partial \phi}{\partial y} \frac{\partial y}{\partial \lambda_2} + \frac{\partial \phi}{\partial z} \frac{\partial z}{\partial \lambda_3} \\ &= \frac{2\lambda_3(\lambda_2^2 - K^2)(K^2 - \lambda_1^2)}{K^2(h^2 - K^2)z} \cdot \frac{\sinh k(s_0 + d)}{\cosh kd} \end{aligned} \quad (83)$$

The nondimensional velocity squared force is then obtained by integrating the summation of the squares over the whole surface. Different components of the force are given as

$$\overline{F_{2\lambda_1}} = \iiint (u_1^2 + u_2^2 + u_3^2) \cos \theta \sin \phi d\lambda_1 d\lambda_2 d\lambda_3 \quad (84)$$

$$\overline{F_{2\lambda_2}} = \iiint (u_1^2 + u_2^2 + u_3^2) \cos \theta \cos \phi d\lambda_1 d\lambda_2 d\lambda_3 \quad (85)$$

$$\overline{F_{2\lambda_3}} = \iiint (u_1^2 + u_2^2 + u_3^2) \sin \theta d\lambda_1 d\lambda_2 d\lambda_3 \quad (86)$$

where,

$$\tan \theta = \frac{\lambda_3}{\sqrt{(\lambda_1^2 + \lambda_2^2)}} \quad \tan \psi = \frac{\lambda_1}{\lambda_2} \quad (87)$$

The integration limits varies for λ_1 from $-a/2$ to $a/2$, for λ_2 from $-b/2$ to $b/2$ and for λ_3 from $-c/2$ to $c/2$, covering the whole domain. On analyzing the force terms it has been found that the λ_1 and λ_2 component of the force have the even function in the integral which due to which on complete integration the force term reduces to zero due to the symmetry of the cross section in any given λ_1 - λ_2 plane . So only λ_3 component of the force contributes to the total velocity squared term. Since the ellipsoid is submerged in the water so there is no interaction with the surface wave due to which the free surface component of the drift force has no contribution. So velocity squared term is the only term contributing to the second order drift force. Due to assumption of no translation and rotation motion, the translation and rotational component are identically zero i.e. $F_3 = F_4 = 0$.

3. IMPLEMENTATION

After solving the boundary value problem to obtain the velocity potential the main task is to calculate the forces by integrating over the surface. As described in Mathematical Formulation, drift forces are calculated using the different geometries using the properties of special function related to the different geometries. Since for some of the geometries it was difficult to calculate the exact closed form solution, a combined solution including analytical and numerical procedure was adopted to obtain the expression for such geometries. The integration for such geometries was carried out first by obtaining a simple form which can be evaluated using numerical integration by discretizing the geometry into small panels. Finally the curves for the drift forces are drawn as the function of ka for the geometries using the MATLAB.

To develop the drift force formulas for the vertical cylinder, the potential function in the cylindrical coordinates was used and the exponential term was expanded using the infinite series of coefficients of the Bessel functions. Bessel functions are the special functions which are obtained when the Laplace equation is solved in the cylindrical coordinates. With the introduction of the Bessel Functions, it became easier to compute a closed form solution for drift force on a cylinder. Using the standard values of these functions graphs were plotted for the dimensionless force term for different values of perturbation parameter ka with an interval of $ka=0.1$.

Similarly the closed form formula for the rectangular body is also calculated. Free surface component is zero in the case of the box so it does not really matter where the

position of the box is with regards to the velocity potential. However, the velocity squared term reduces to a very simple closed form formula independent of ka which can be used to calculate the second order drift force. For the deep water it has been assumed that $d \gg D$, due to which hyperbolic sine term containing the d reduces to 1 and a new version of the formula is obtained independent of d .

To decrease the complexity in the integration and evaluation of forces, cylindrical coordinates are introduced for analyzing horizontal cylinders. With the introduction of the cylindrical coordinates the computation of the integration over the domain becomes much simpler in the case of horizontal cylinder and half cylinder, leading to a compact form of the integral. Further the integral was solved using the numerical code, in which the whole surface was divided into the small strips subtending an angle of $d\theta=1^\circ$ at the center. The integration was carried out using MATLAB. Finally a formula was developed in terms of the integrand $I'(ka, s_0/d)$ for cylinder and $I'(ka)$ for half cylinder which can be obtained from the values given in the Table 1 for different ratios of submergence depth to the water depth.

As in the case of the horizontal cylinder, cylindrical coordinates are used in formulation of the drift forces on a half cylinder. The velocity squared term is integrated over the whole surface using the similar procedure of dividing the surface into small strips subtending an angle $d\theta=1^\circ$. The integration was done using the MATLAB code and the formula for the drift force was developed in terms of the integrand $I'(ka)$ which can be obtained from Table 1 for different values of ka .

Spherical coordinates are used in the formulation of the drift forces of hemisphere and sphere. The potential function is obtained in the spherical coordinates which is then differentiated to generate velocity components. The velocity squared term is further simplified and an integrand is obtained in terms of hyperbolic and trigonometric functions of ka , θ and μ . The integration is carried out over the surface of the hemisphere by dividing the whole surface into strips subtending angles of 1° at the centre. The graphs for the dimensionless force are developed for different values of ka which can be used to calculate the second order drift forces for a rigid hemisphere. In the case of the submerged sphere, again the spherical coordinates were used for the formulation of the drift forces. To calculate the velocity squared term the integration is carried out using the same technique. For the case of sphere, one can also calculate the forces by introducing the Legendre polynomial like Bessel function in vertical cylinder, but because of the complexity involved in their simplification this approach have not been carried out in this study.

In the case of ellipsoid, the potential function in the cartesian coordinates is used which is then differentiated with respect to the ellipsoidal coordinates using MAPLE and the differentiation was also verified using hand calculations. Finally a simpler integrand was evaluated which was solved using the same technique as used for the sphere and cylinder by dividing the surface into small strips here of $d\lambda_1$, $d\lambda_2$ and $d\lambda_3$, where $d\lambda_i$ s are of unit length. However, one can approach the solution by the introduction of the Lamé functions which are the solutions of the Laplace equation in the ellipsoidal coordinate. Generally these functions are used in the electrostatics to calculate the potential around ellipsoidal source field. Punzo et.al [34]. In the similar fashion potential function around an ellipsoidal body can be calculated to derive the second order drift forces. But, due to the appearance of the singularity while integrating this approach is not used in this study and the other approach as defined before is preferred.

4. STEADY DRIFT FORCE NUMERICAL EXAMPLES

4.1 Basic Body Geometries

The graph showing the variation of drift force for vertical cylinder for different water depths has been shown in the Fig. 8. For the vertical cylinder it has been found that the free surface component is independent of water depth while the velocity squared term of the drift force is a weak function of water depth at lower values of ka . With the increase in the value of the ka , total drift force increases but the rate of increase of the total drift force decreases with the increase in the value of ka specially for $ka \geq 1.5$. The presence of Bessel function of the second kind in the velocity squared term explains the increase of the velocity squared term with the increase in the value of ka .

In the case of rectangular box, interestingly the mean of free surface component comes out to be zero. Also, it is interesting to note that the final non dimensional term for velocity squared component is independent of the geometry of the box and is dependent on the water depth only.

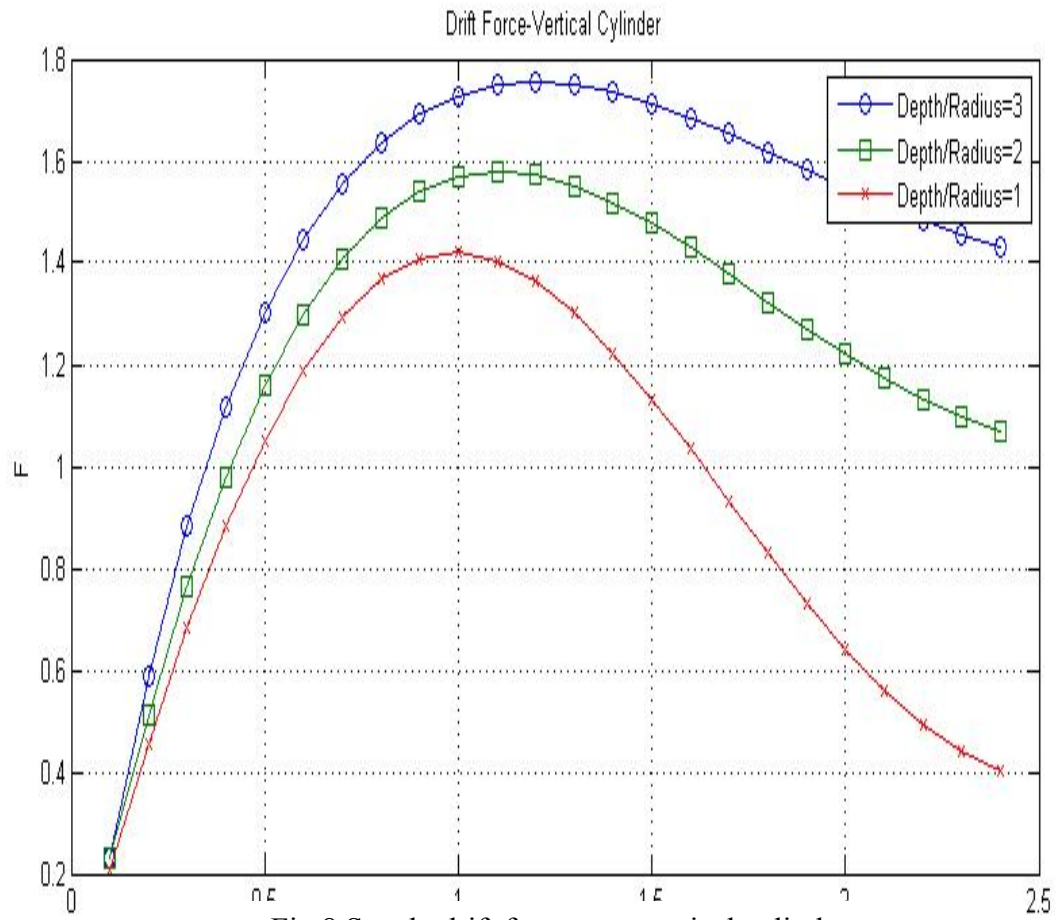


Fig.8 Steady drift force on a vertical cylinder

In the case of the horizontal cylinder, the free surface component is not present as the body is submerged into the water however the velocity squared terms has a significant effect which should be accounted. The drift force peaks at intermediate ka values and after that non dimensional force term decreases drastically with the increase in the ka value as shown in Fig. 9. For depth, 3 times of the radius value the force is almost negligible for $ka \geq 1$. As expected the drift force decreases with the increase in the depth of submergence, which can be explained by the decrease in magnitude of the velocity as one moves down to the sea bed. Also as discussed in the derivation horizontal component of the drift force is equal to zero accounting for the symmetry of the shape.

Horizontal half cylinder also have no free surface effect as it is submerged completely in water and seated on the sea bed. The results as shown in Fig. 10 shows that velocity squared component is significant with the lower ka values and goes on decreasing with the higher values of ka . For lower water depths force is negligible for $ka \geq 1.5$. The results show a continuous increase in the force with the decrease in the water depth.

In the case of the bottom mounted hemisphere horizontal and vertical force peaks at an intermediate value (Fig. 11). The magnitude of the force has shown decreases with the increase in the water depth similar to other geometries. Because of the deep submergence in the water, the free surface effect is not applicable in this case also.

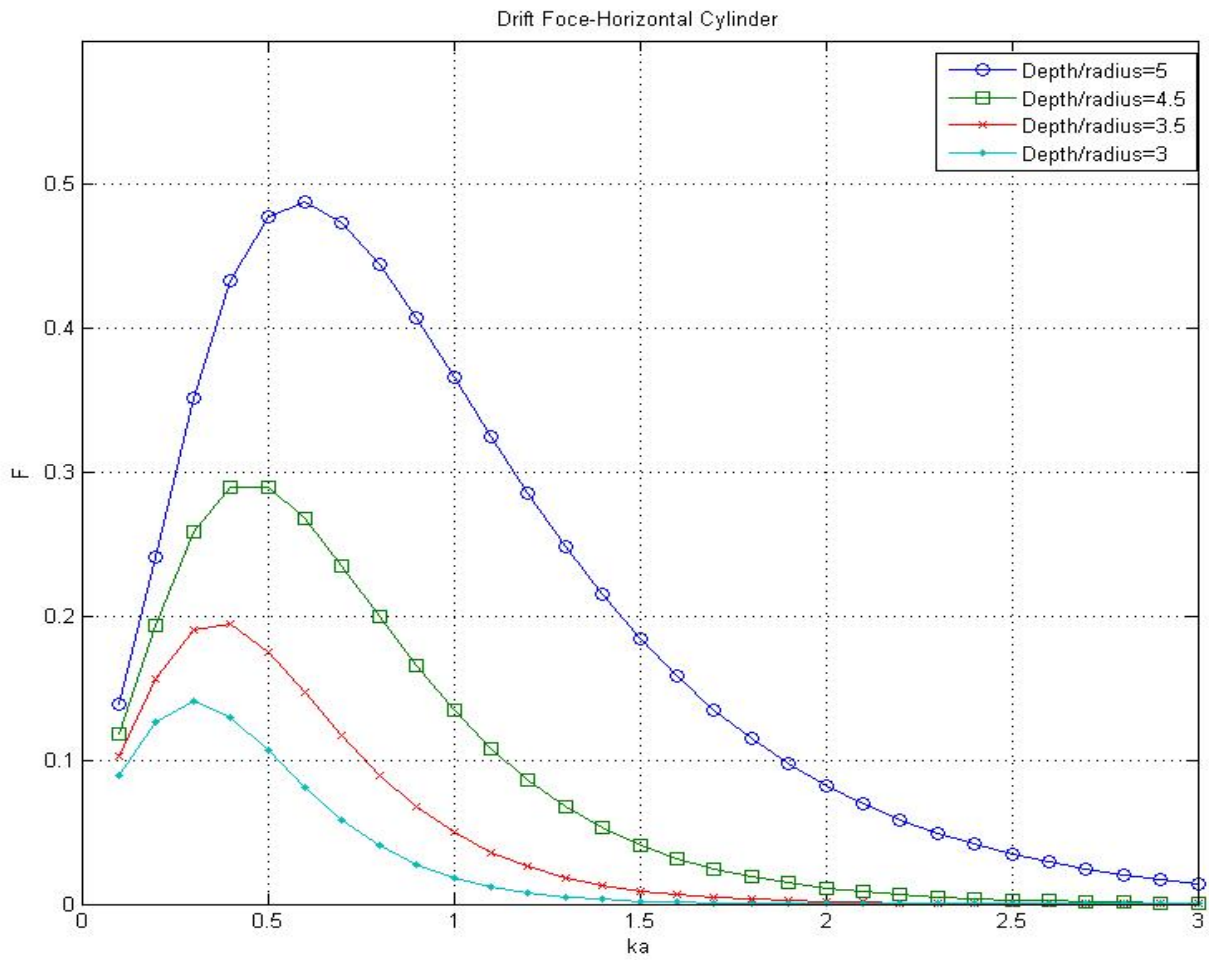


Fig.9 Steady drift force on a horizontal cylinder

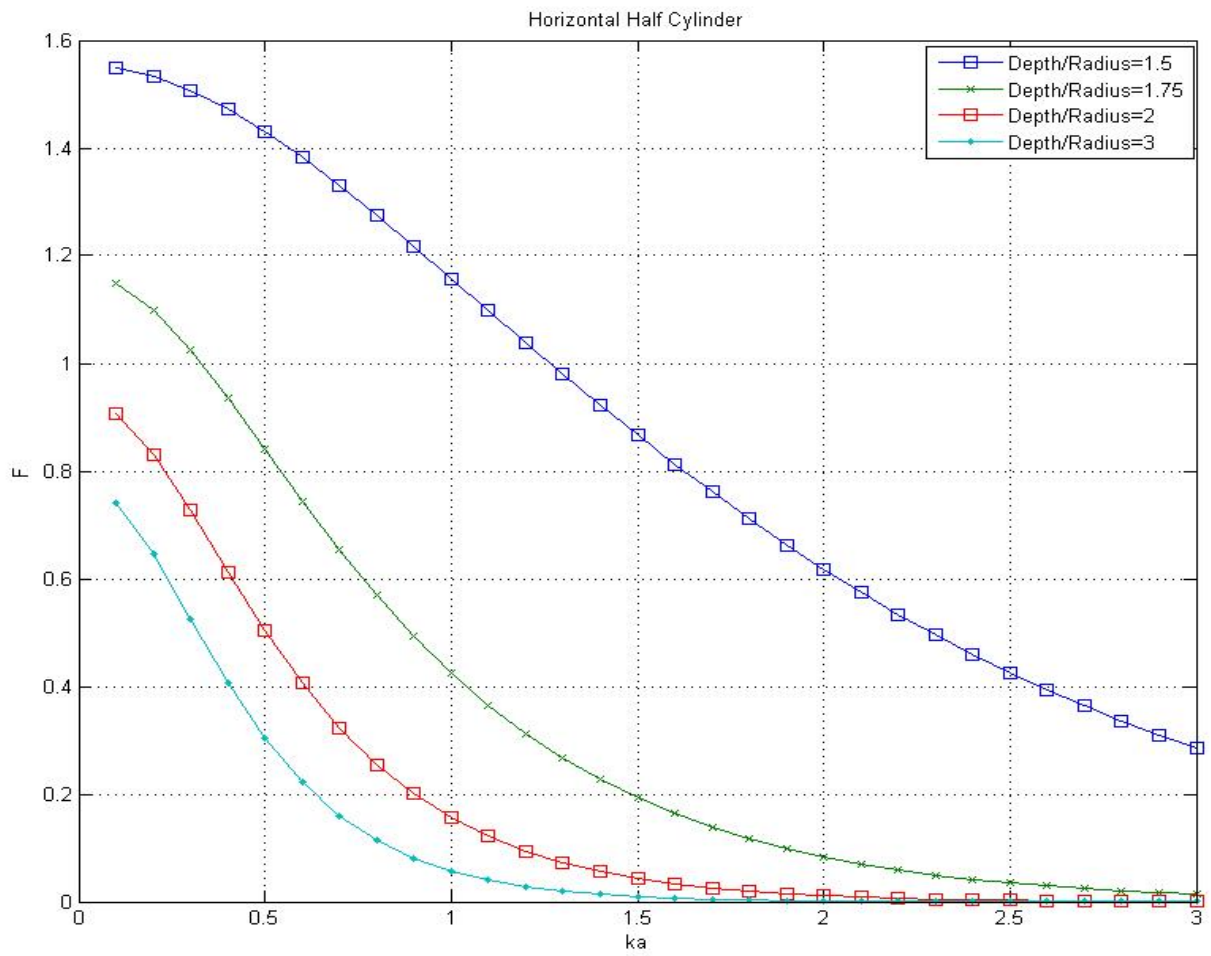


Fig.10 Steady drift force on a horizontal half cylinder

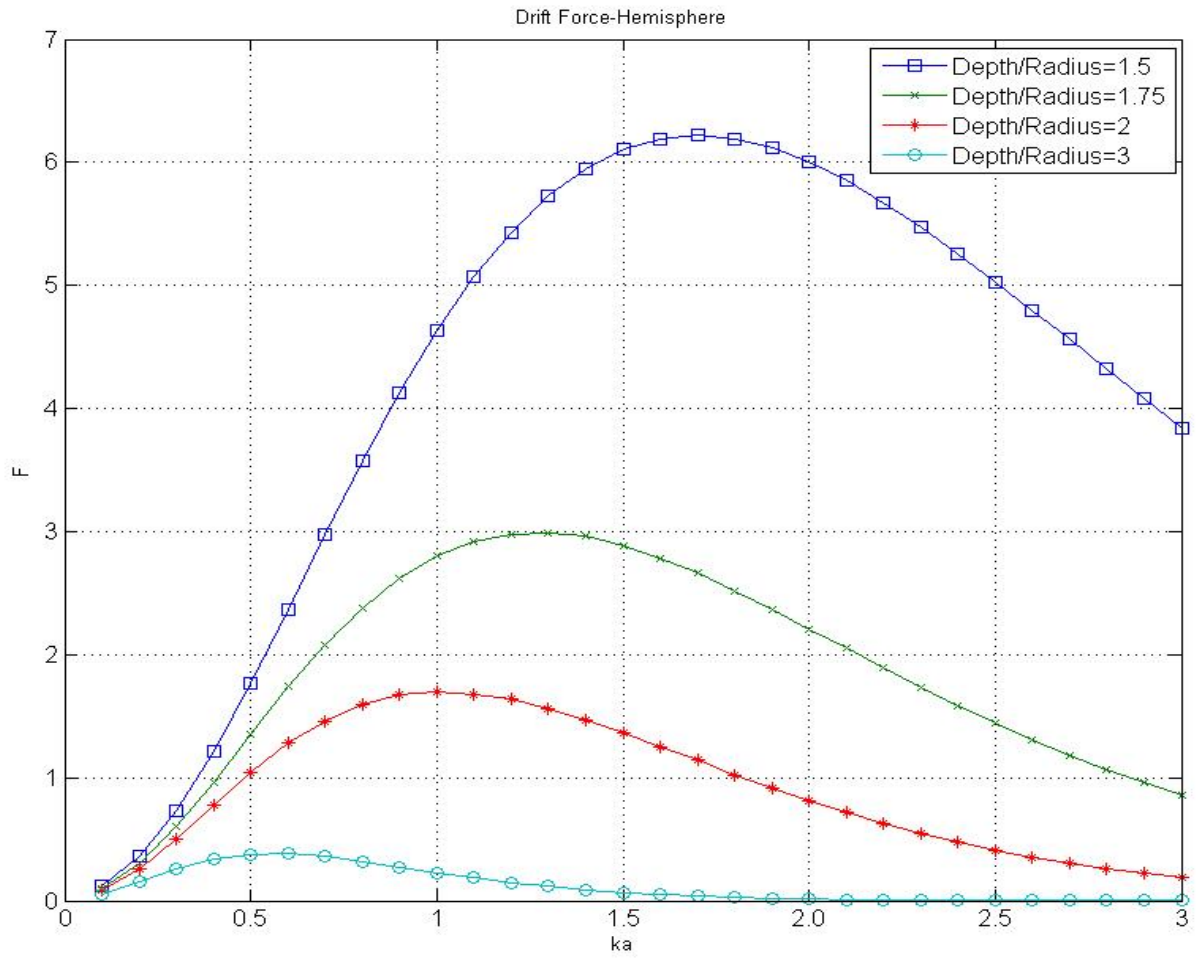


Fig.11 Steady drift force on a hemisphere

The velocity squared results for the sphere submerged in water with different water depths have been calculated keeping the ratio of depth of submergence to the radius as a constant parameter. The results showed (Fig. 12) that as the water depth increases the mean drift force decreases. Also, drift force peaks for intermediate value of ka showing almost similar trend as shown by hemisphere. The higher values of ka the force almost approaches to zero. Also it is seen that as the sphere comes closer to the surface the drift force increases as can be seen by the plot.

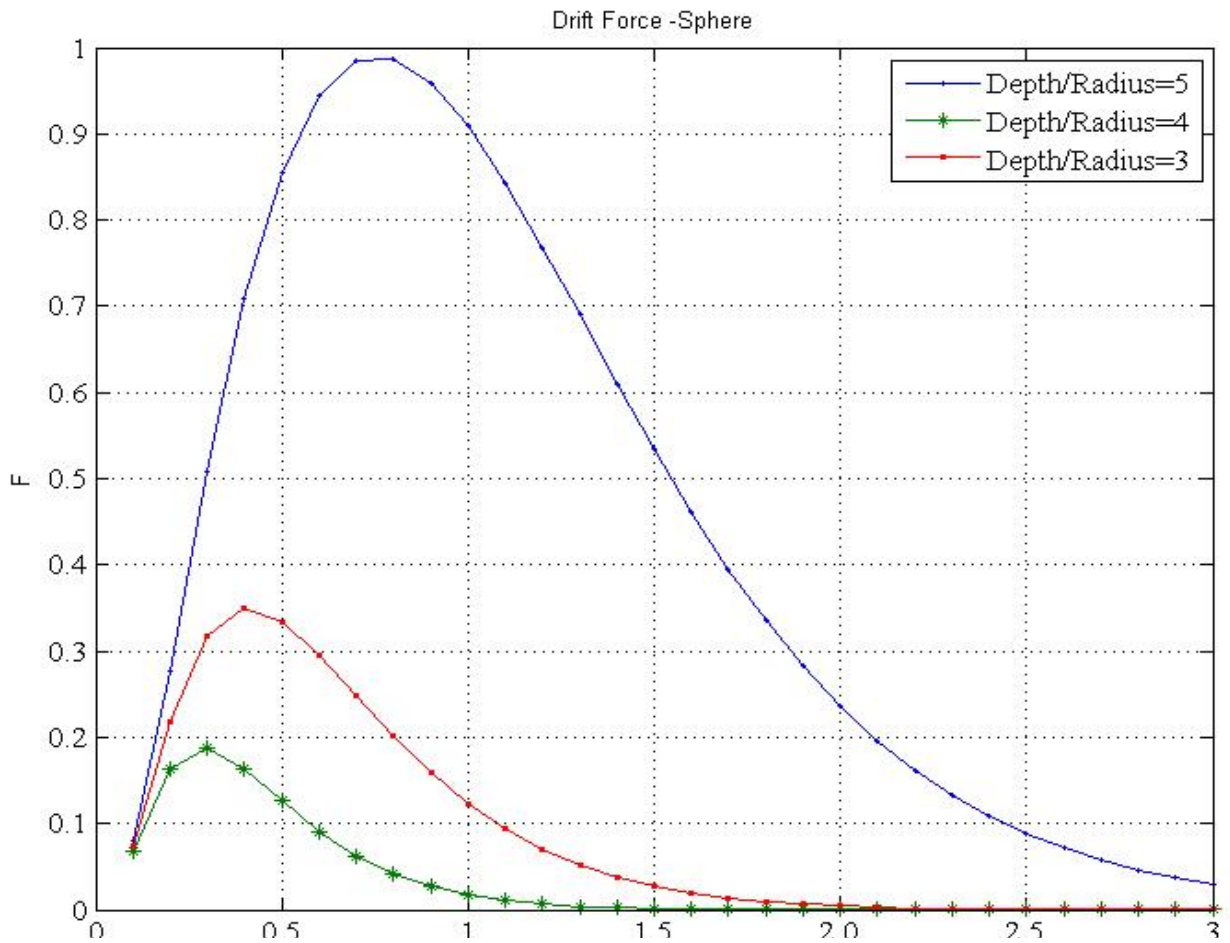
In the case of submerged ellipsoid the ratio of the different axial lengths (a,b,c) effects the drift force significantly. A sharp peak has been observed in the intermediate ka values as can be seen from Fig. 13. It can be seen from the result when any of the minor axis decreases in size with respect to measure axis or in other words ellipsoid squeezes and becomes more slender, drift force on the body decreases. Thus, one can conclude that the slender body faces less drift force which can explain the natural design of the body of the fish.

The results for equal axial length cannot be calculated because of the presence of the singularities in the velocity squared force term (eq(18)). . However, to check for the ellipsoid the axial length were made as close as possible to avoid singularity and it has been found that the results (Fig. 14) obtained are approaching to the results obtained for sphere. The convergence of the results has been shown in the Fig. 14. Lower values of the ellipsoids as compared to the sphere can be explained for the fact that the ellipsoid is

having lower surface area as compared to sphere as minor axes of the ellipsoid are smaller than sphere.

As discussed with numerical examples use of these formulas and charts make calculation of drift forces very simple as compared to the time consuming numerical techniques. As most of the structures in offshore industry have these basic shapes as their components, designers can get a quick idea of the forces coming over structure, which will increase the speed and accuracy.

a)



b)

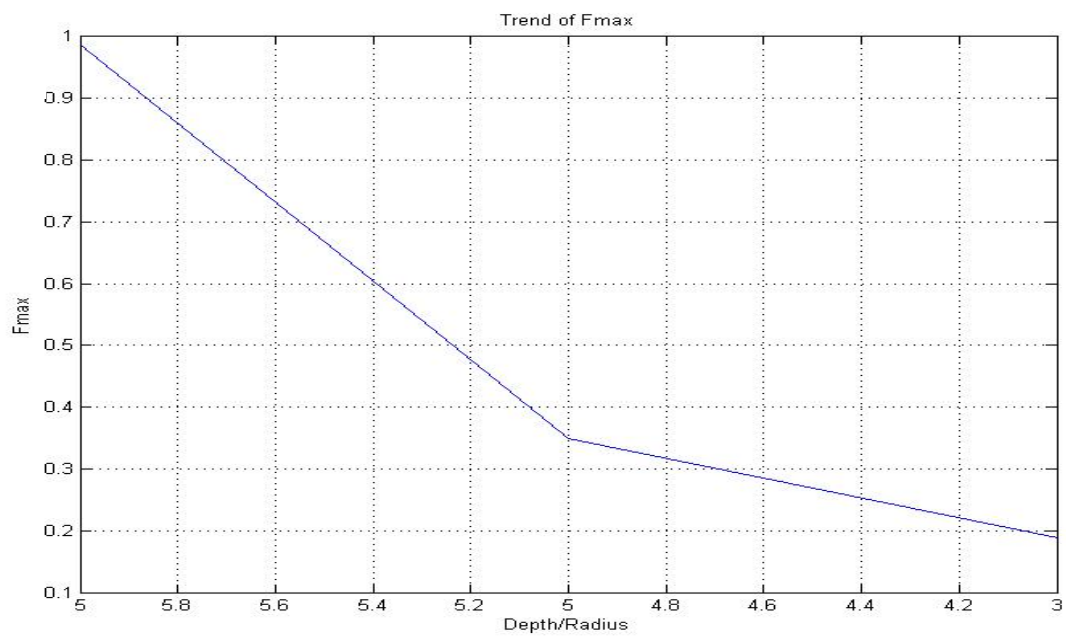


Fig.12 a) Steady drift force on a sphere
b) F_{max} values of sphere

a)

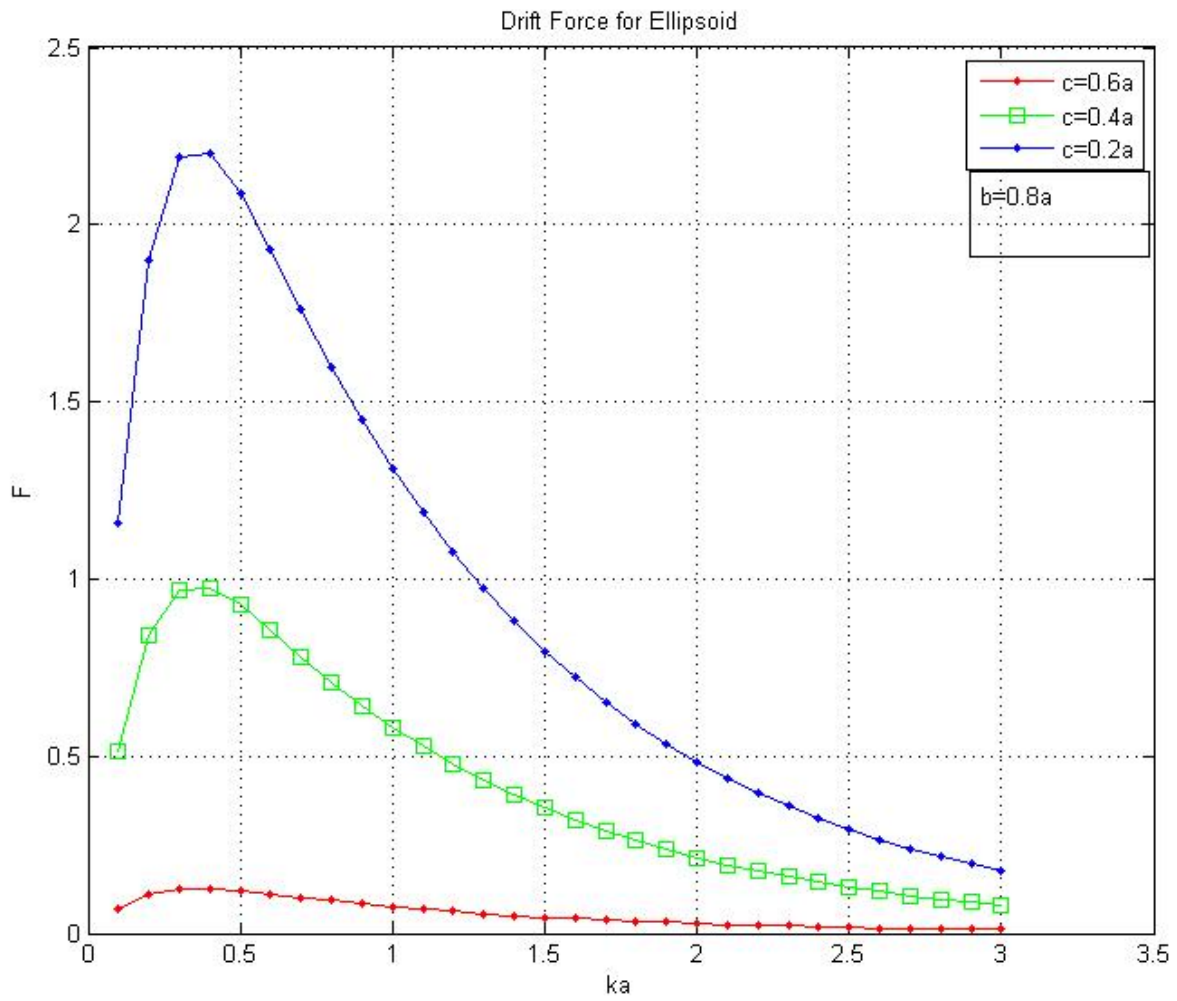


Fig.13 a) Steady drift force on an ellipsoid with constant a and b
 b) steady drift force on an ellipsoid with constant a and c

b)

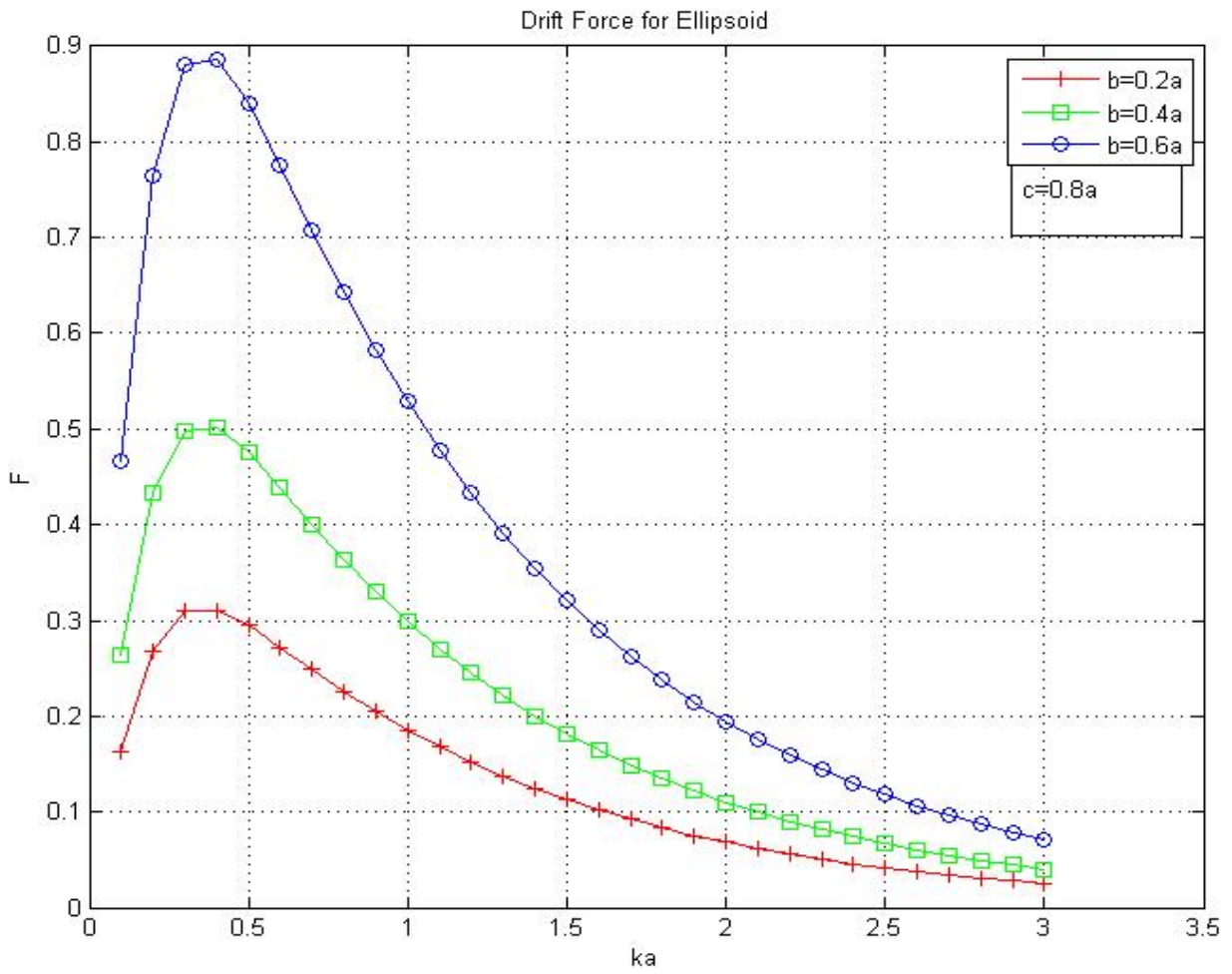


Fig. 13 continued

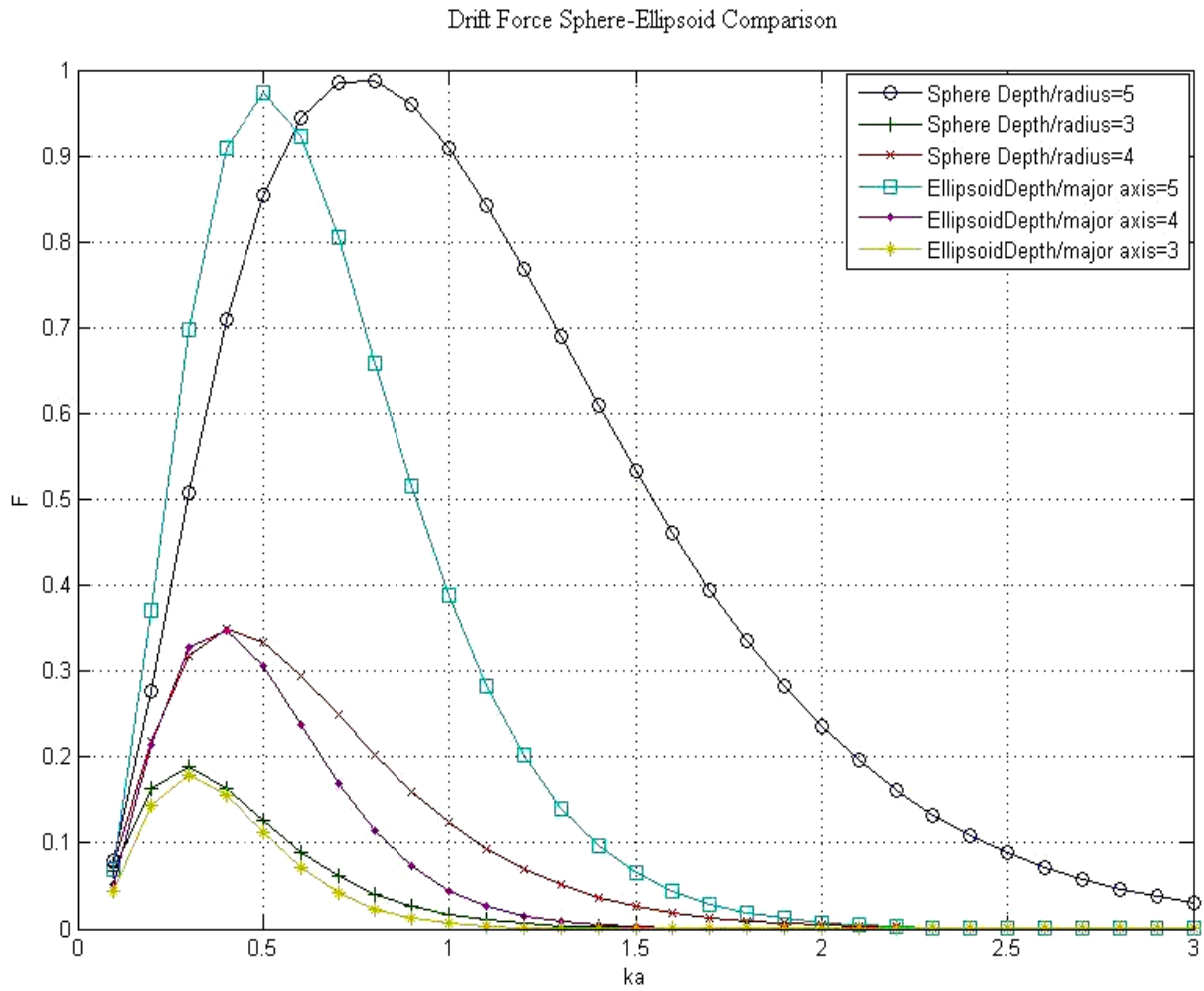


Fig.14 Comparison of sphere and ellipsoid results

4.2 Effect of Neglecting Translation and Rotation Contribution

4.2.1 Barge

To illustrate the mathematical formulation for the rectangular bodies, an example of a barge is presented here. The results obtained for the barge are compared with the results from Choi et al. [7]. The properties of the barge are defined in Table 2. The barge taken for the example is similar to the example used by Choi et al. [7]. The results are presented in Fig. 15. The dimensionless drift force is plotted against the frequency ω .

Choi et al. [7] used four different discretization to analyze the structure using the HOBEM method (Higher Order Boundary Element Method) accounting for the free surface, velocity squared and motion terms. They found that the total force first increases suddenly at certain value frequency ω which is then almost constant for all higher values of frequency ω .

Dispersion relationship, eq (39) is used to plot the force against frequency as force is the function of wave number, k , only as described in the mathematical formulation. The initial disturbance in the values can be accounted for the exact determination of the wave number, which requires iterations to reach the exact value. A graph of the ratio (p) of the velocity squared term and free surface term (F_1+F_2) to the total force ($F_1+F_2+F_3+F_4$) is plotted against frequency ω . Since free surface effect is zero in case of rectangular bodies, the ratio p reduces as follows

$$p = \frac{F_1 + F_2}{F_1 + F_2 + F_3 + F_4} \quad (88)$$

which is equivalent to:

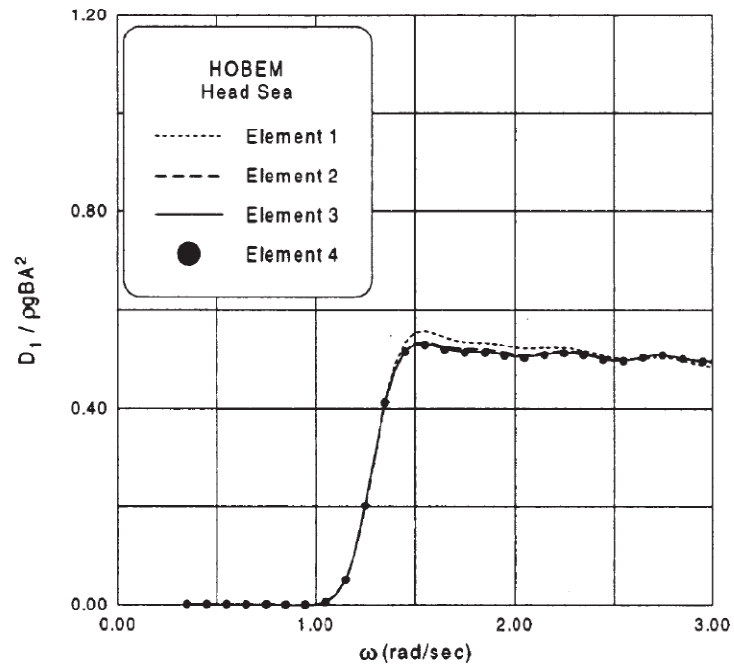
$$\frac{F_2}{F_2 + F_3 + F_4}$$

Form the results it has been concluded that for lower value of frequency ratio of velocity squared term to total force is very small which increases and approaches towards total force for higher frequencies or lower period waves. So, it can be concluded that for the lower period waves, velocity squared term is the main contribution in total drift force.

Table 2 Properties for Barge Example

Property	Value
Length	30 m
Breadth	22 m
Draft	1.5 m
Water Depth	15 m
Displacement	990 m ³

a)



b)

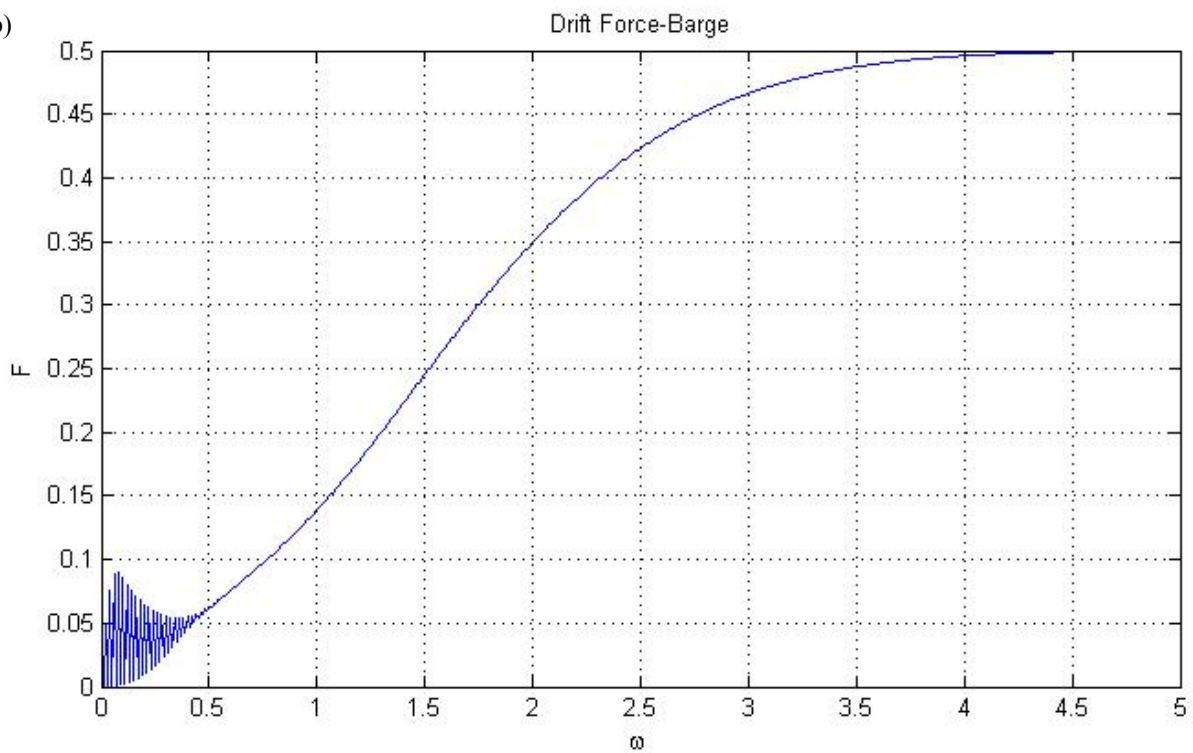


Fig.15 (a) Graph from Choi et al.[7]
 (b) Validation of barge example with Choi et al. [7]
 (c) Comparison of free surface and velocity squared component with total force from Choi et al. [7]

c)

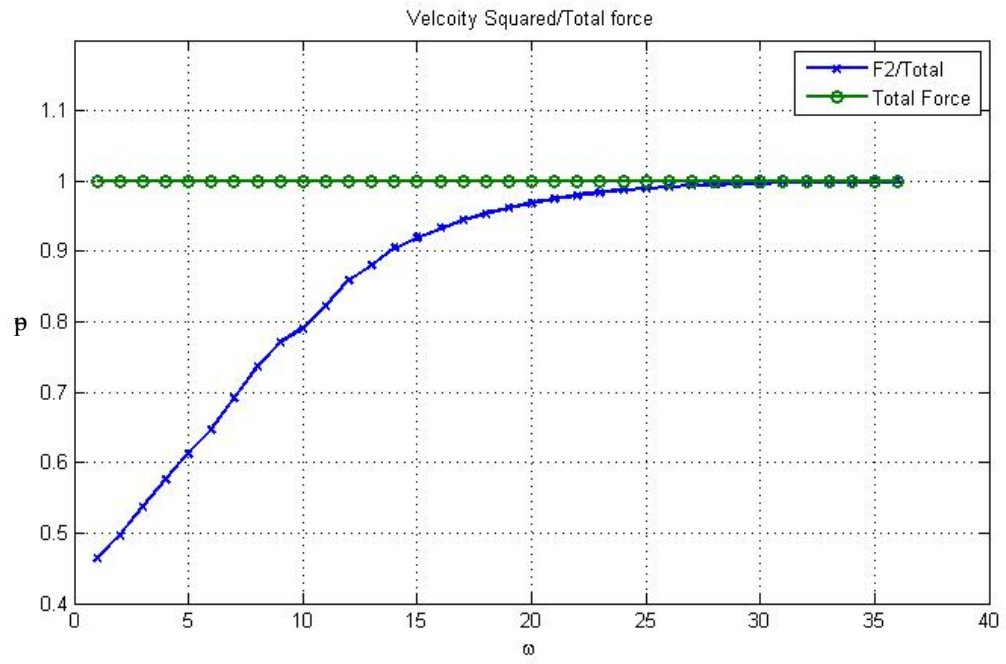


Fig. 15 continued

4.2.2 Sphere

To illustrate the importance of the velocity squared term a comparison has been made between velocities squared term and the total force using the example of a submerged sphere. The trend of results obtained for the sphere is in agreement with the one obtained by Wu.et.al [39] as shown in Fig. 16. The difference in values can be accounted because of assumption of no translation and rotational motion effect in analysis. A ratio of total force is shown in Fig.16 which shows that the velocity squared is the main component of the drift force and contributes to 60-80% of total force.

a)

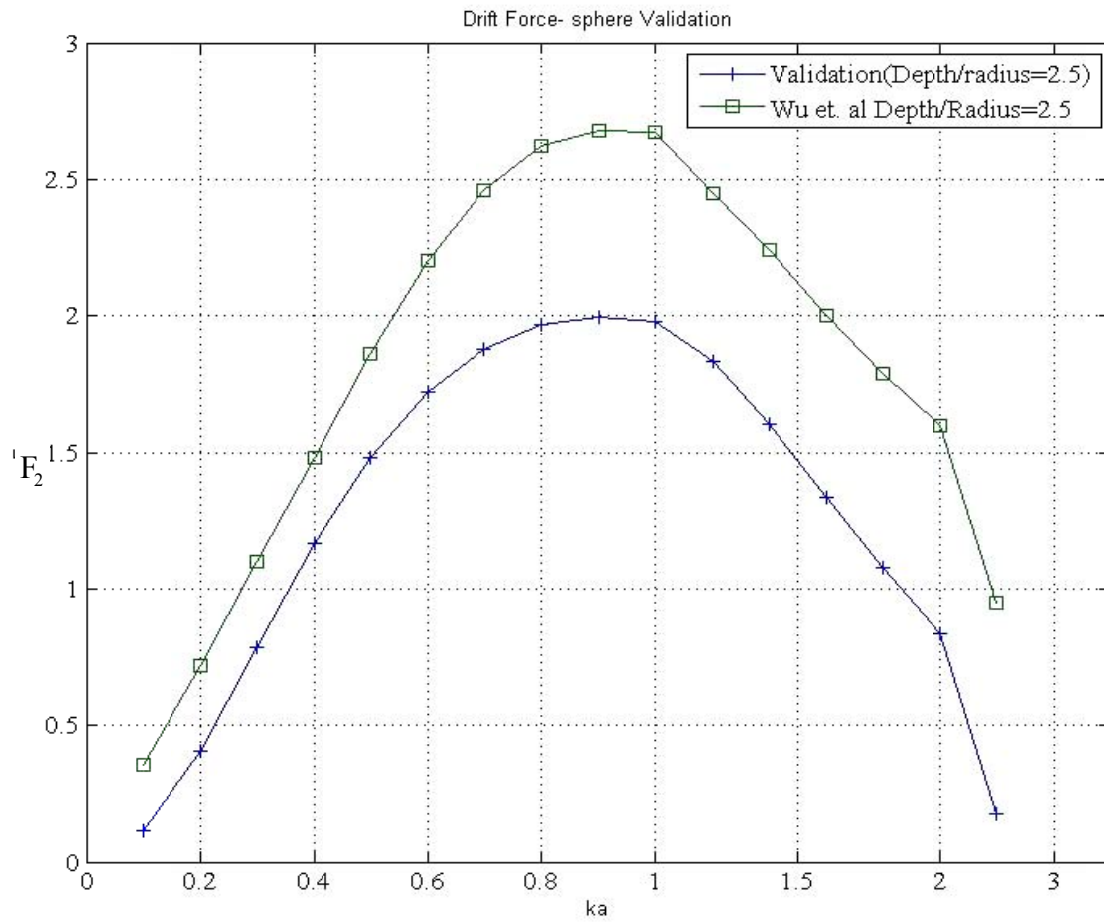
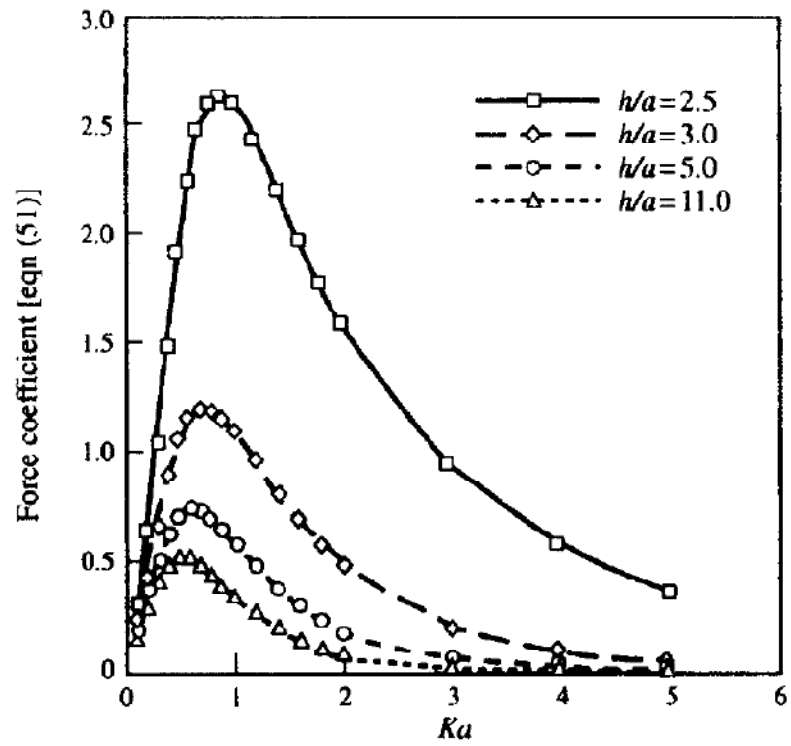


Fig. 16 (a) Validation of sphere result with Wu et al. [39]
 (b) Graph from Wu et al. [39]
 (c) Ratio of velocity squared term to total force

b)



c)

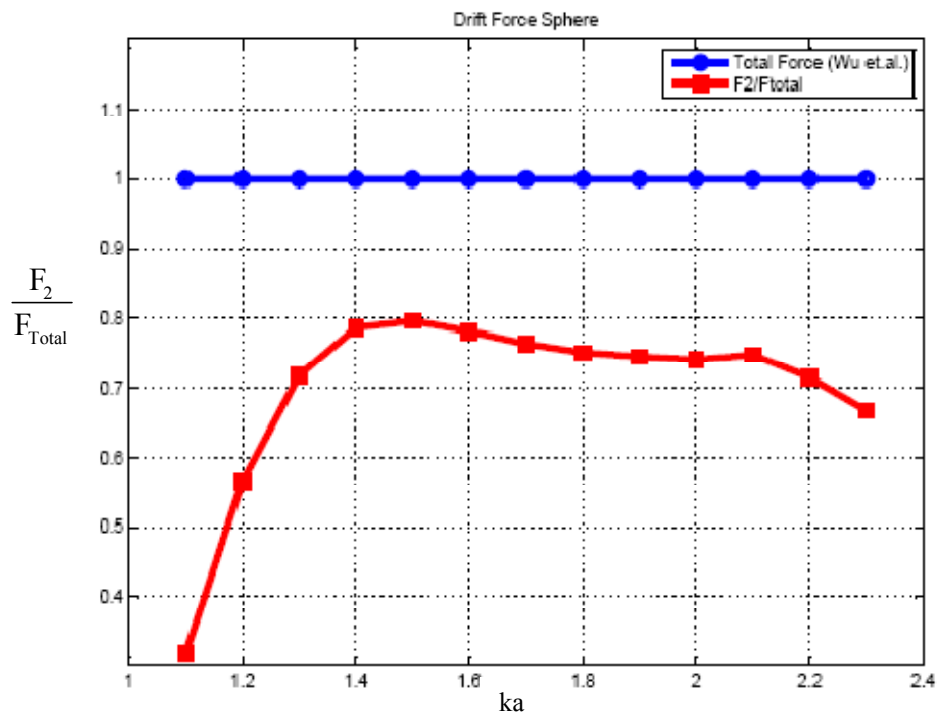


Fig. 16 continued

4.3 Approximations Using Ellipsoidal Geometries

4.3.1 Autonomous Underwater Vehicle (AUV)

To demonstrate the formulation for the ellipsoid, an example of the Autonomous Underwater vehicle (AUV) is taken which was published by Wang et al. [37]. The geometry has been described in the Table 3 and the geometry of the structure is described in Fig. 17. Since the calculation of the exact geometry is not possible, so the given AUV is approximated to an ellipsoid using the two approaches and an envelope is constructed.

1) Equivalent Area Method

The areas of the cross-sections of AUV as shown in the Fig. 17 were compared to the cross-section of an equivalent ellipsoid to obtain the axial lengths keeping the major axis as the overall length of the AUV as shown in Fig. 17. The approximate area of the cross-sections is calculated by dividing the geometry as shown in Fig. 17.

Horizontal Plane

The approximate area for the cross-section along horizontal plane was calculated which is equal to 1458.54 cm^2 . Now this area can be equated to the area of ellipse ($\pi ab/4$) to obtain the horizontal minor axial length.

Longitudinal Plane

The approximate area for the cross-section along vertical plane was calculated which is equal to 9040 cm^2 . Now this area can be equated to the area of ellipse ($\pi ac/4$) to obtain the vertical minor axial length.

Since maximum dimension in direction of major axis is 200, we assume $a=200$ cm

By equating the areas we get, $b = 92.7$ and $c = 57.56$ cm

So the ratio of the axial lengths is $a:b:c=1:0.4635:0.2878$

2) Maximum Lengths

According to this approach maximum lengths in both the cross-sections are taken as the axial lengths so $a=200$ cm, $b =100$ cm, $c =60$ cm and thus the ratio $a:b:c=1:0.5:0.3$.

Drift force acting on the geometry will lie within this envelope, thus giving us a range of drift force acting over the given geometry. It can be seen from the plot that the force peaks for intermediate values of ka similar to the sphere. Also for higher values of ka , the drift force is almost negligible. This example illustrates that how one can calculate the range of the drift force acting on a geometry that can be approximated as an ellipsoid. Similarly different shapes can be approximated into other geometries and results can be calculated faster and easily.

Table 3 Properties for AUV Example

Property	Value
Length(Body/Overall)	2/2 m
Breadth (Body/Including Elevator)	1/1.6 m
Height (Body/Including Vertical Fins)	0.6 /0.6 m
Displacement	990 m ³

a)

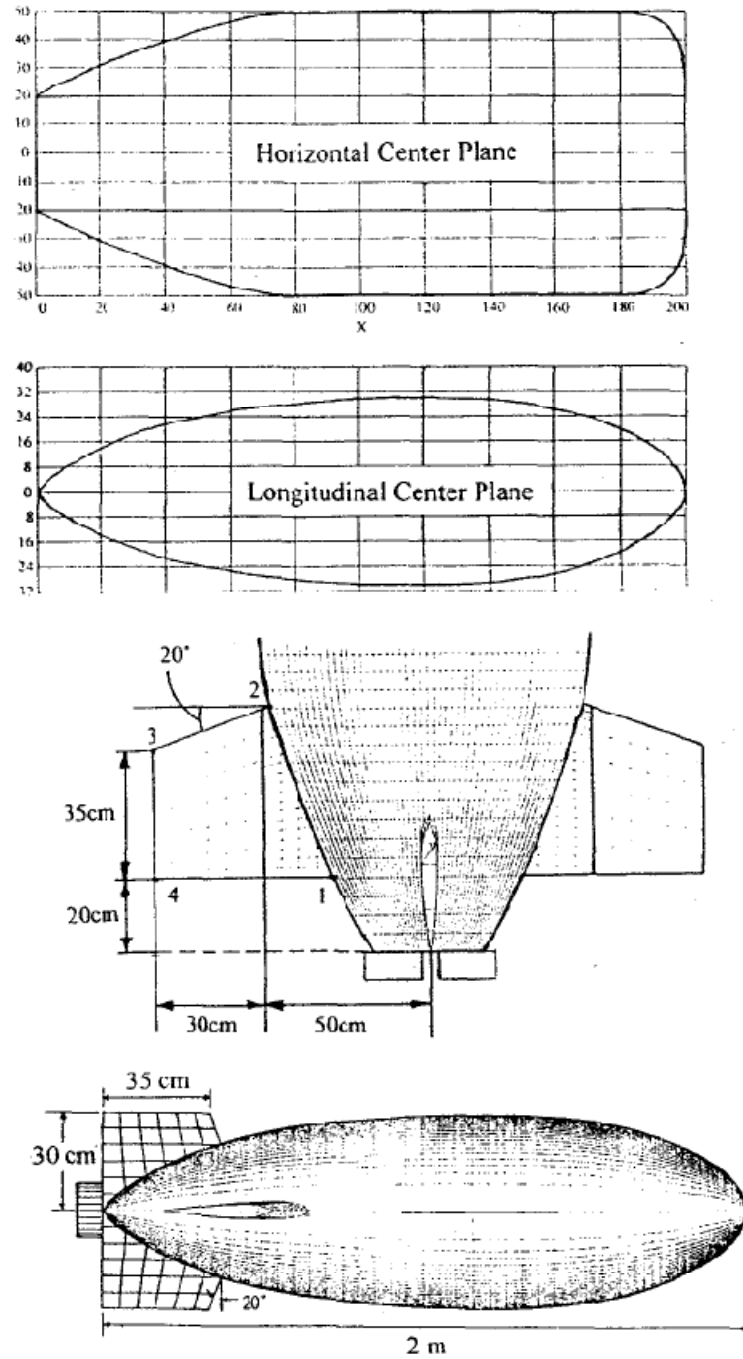


Fig.17 a) Description of AUV example (Wang et al.(49))
 b) Different areas of cross-section
 c) Drift force on AUV

b)

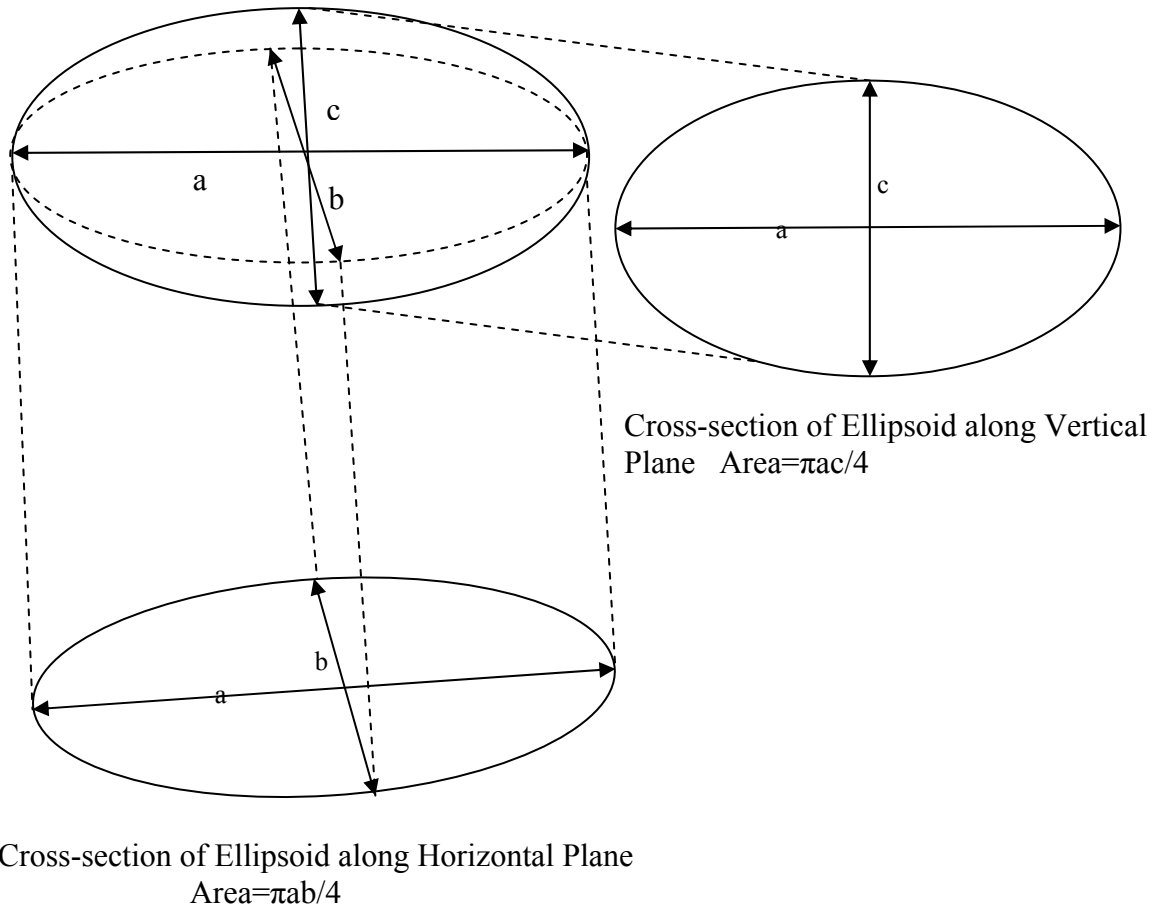


Fig. 17 continued

c)

Drift Force for AUV

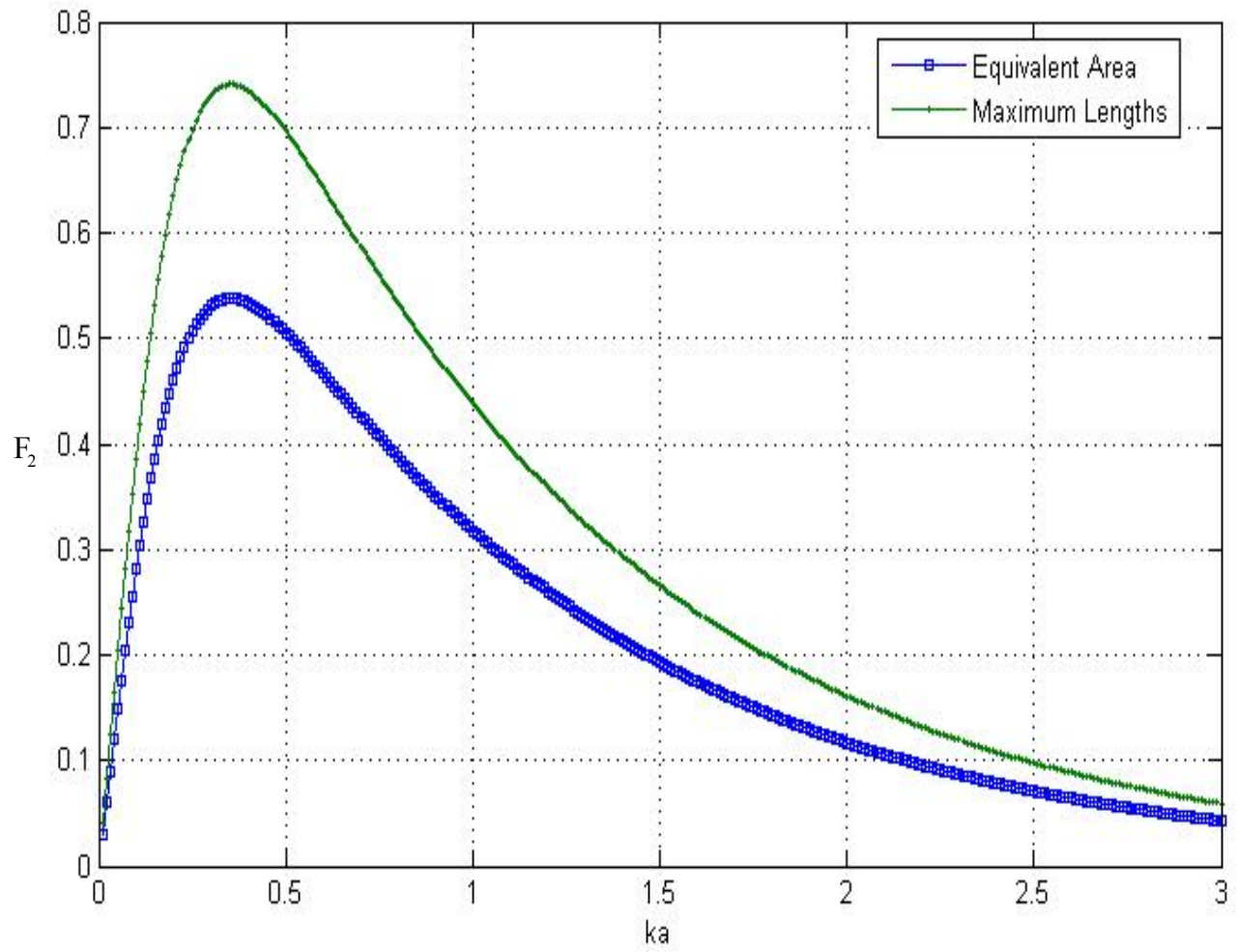


Fig. 17 continued

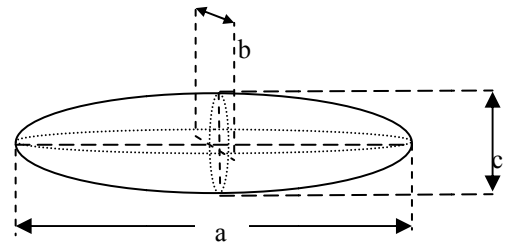
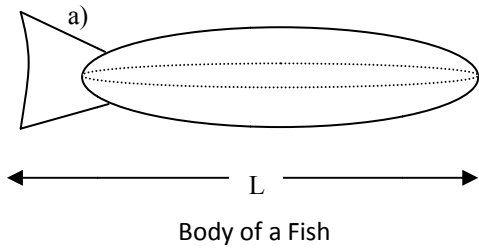
4.3.2 Fish

To illustrate a real life example, an example of a fish body is considered which is approximated as an ellipsoid. The drift forces acting over body of different fishes have been shown in the graph (Fig. 18), which proves that slender body of a fish face very less load as compared to other structure. The fish body has been assumed as an ellipsoid with the major axes $a=0.93L$, $b=0.195L$ and $c=.112L$, where L is the overall length of the fish. This is a reasonable assumption for the dimension for dorsal, lateral, and head aspect, but less accurate with tail aspect of fish.(Haslett[13]).

The different fishes considered for analysis with their respective overall lengths are given in Table 4. It can be concluded from the graph that the longest fish is having maximum force which is expected as the longest fish will have the maximum surface area for the same ratio of the axes.

Table 4 Overall Lengths of the Different Fishes (Haslett [13])

Fish	Length
Cod	120 cm
Haddock	60 cm
Herring	30 cm
Spart	15 cm



Approximation as an Ellipsoid
 $a=0.93L$, $b=0.193L$, $c=0.112L$


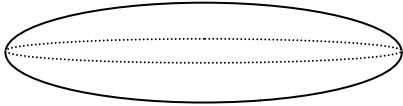

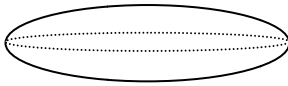

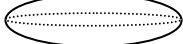

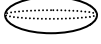
Fish	Geometrical Approximation
 Cod	 $L = 120 \text{ cm}$
 Haddock	 $L = 60 \text{ cm}$
 Herring	 $L = 30 \text{ cm}$
 Sprat	 $L = 15 \text{ cm}$

Fig. 18 a) Geometrical approximation of different fishes
 b) Drift force on fishes

b)

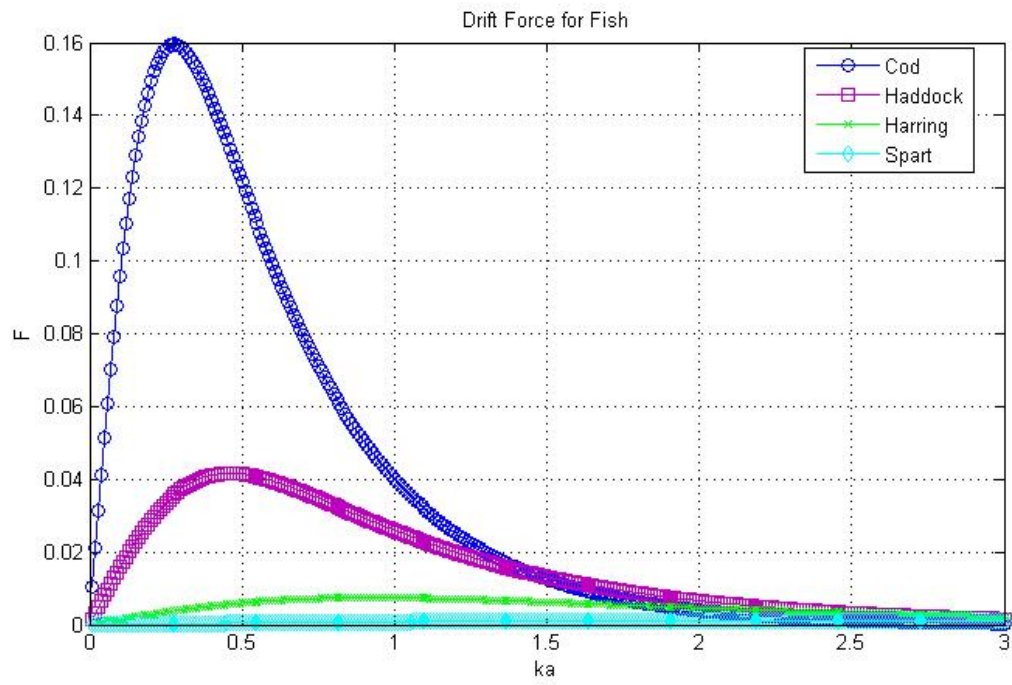


Fig. 18 continued

5. SUMMARY AND CONCLUSIONS

The research study presented here was started with the basic geometries of the cylinder and hemisphere, the results of which were published in Chakrabarti and Gupta [5]. This study was then extended to ellipsoidal and spherical bodies which are mainly the focus of the thesis.

Wave force on a body can be obtained using approaches depending on the type of fluid flow (viscous or inviscid), on the characteristic dimension of the structure relative to the wavelength. Morrison equation provides the empirical expressions for the wave force on the body which involves experimentally obtained drag and inertia coefficients. The validity of the Morrison equation is limited to the structures whose characteristic dimension is less than wavelength due to occurrence of diffraction and radiation effects. In this case it is recommended to use the diffraction theory which accounts for both incident and diffracted potential which is obtained by solving Laplace equation in the given boundary conditions. The solution of the Laplace equation can be of n^{th} order. However, larger order terms generally have negligible effects so research is generally focuses up to second order forces.

Second order drift force which is the main focus of the study here, comprises of the free surface structure interaction, velocity squared component from the Bernoulli's equation, translation and rotational term accounting for the motion of the structure. This work concentrates only on free surface and the velocity squared components. One can obtain the translational and rotational term if the motion of the structure is provided.

However, it has been shown by comparison with the total force that the velocity squared term is the main component and accounts for the 60-80% of the total force. For shorter period wave the contribution of the velocity squared term increases significantly.

Numerical techniques available for the solution of the second order wave forces generally require complex computations, due to which a need of quicker estimates arises as emphasized by Newman [29] and Faltinsen [9]. The analytical and hybrid of analytical and numerical methods developed here provides a much simple analysis. Laplace Equation is solved and the velocity potential is obtained in different coordinates system due to which the expression of force can be obtained in terms of special functions like Bessel function and integrands which are easy to calculate. Also with certain examples it has been shown how one can attempt to bound the actual results by approximating the complex structure into simpler geometries greatly simplifying the problem in to have quick estimates of second order forces.

From the study it has been concluded that the velocity squared component and the free surface component forms the major part of the second order drift force in the case of the sphere and barge. Also, studies shows that the complex structure can be approximated into simpler geometries to get quick first pass estimates of second order analysis.

REFERENCES

- [1] Abramowitz M, Stegun IA, Handbook of Mathematical Functions, Dover Publication, New York, 1972.
- [2] Black L, Wave forces on vertical axisymmetric bodies. Journal of Fluid Mech. 1975, 67: 369-376.
- [3] Bora SW, Hydrodynamic coefficient for water wave diffraction by spherical bodies, Sadhana, 29 (6): 617–628.
- [4] Chakrabarti SK, Hydrodynamics of Offshore Structures. Computational Mechanics Publications, London, 1987.
- [5] Chakrabarti S, Gupta A, Steady wave drift force on basic objects of symmetry. In: 4th International Fluid-Structure Interaction Conference, 92:1-11, 2007.
- [6] Chakrabarti, SK, Naftzger, RA, Nonlinear wave forces on half cylinder and hemisphere, Journal of Waterways, Harbors and Coastal Engineering Division, ASCE 1974; 100:189-200.
- [7] Choi YR, Hong SY, Choi SH, An analysis of second order waves forces on floating bodies using higher order boundary element method, Journal of Ocean Engineering, 2000, 28:117-138.
- [8] Faltinsen OM, Sea loads on ships and offshore structures, Cambridge Ocean Technology Series, 1998.
- [9] Falteinsen O, Loken A, Drift forces and slowly-varying horizontal forces on a ship in waves. In: Proc. Symposium on Applied Mathematics, paper no.2241, 1978.
- [10] Faltinsen O, Michelsen F, The motion of large structures in waves at zero Froude number. In: Symposium on the Dynamics of Marine Vehicles and Structures in Waves, 91–106, 1974.

- [11] Fenton JD, Wave forces on vertical bodies of revolution. *J. Fluid Mech.*,1978,85: 241-255.
- [12] Garrison C.J, Rao SV, In:Interaction of waves with submerged objects. *Journal of Waterways, Harbors and Costal Engineering Division ASCE*, 1971, 97: 259-277.
- [13] Haslett RWG, Measurment of the Dimension of Fish to Facilitate Caculations of Echo-Strength in Acoustic Fish Detection, lecture to acoustics Group of Physical Society,1960
- [14] Havelock TH, Waves due to a floating sphere making periodic heaving oscillations. In:.,*Proc. R. Soc.*, 231: 275–285, 1955.
- [15] Hermans AJ, Lisette M, Sierevogel, A discussion on the second order wave forces and wave drift damping, *Applied Ocean Research*, 1996, 18: 257-263.
- [16] Kim MH, Yue DKP, The complete second-order diffraction solution for an axisymmetric body. Part 1. Monochromatic incident waves. *Journal of Fluid Mechanics*, 1989, 200: 235-264.
- [17] Kokkinowrachos K, Mitzlaff A, Zibell H, Verhalten von Mehrkörpersystemen bei Operationen im Meer. In: *Jahrbuch der Schiffbautechnischen Gesellschaft*,80: 341–364, 1980.
- [18] Li W, Williams AN, The diffraction of second-order bichromatic waves by a semi-immersed horizontal rectangular cylinder. *Journal of Fluids and Structures*, 1999, 13(3): 381-397.
- [19] Longuet-Higgins HC, Prazdny, K., The interpretation of moving retinal images. *Proceedings of the Royal Society of London B*, 208:385–387, 1980.
- [20] MacCamy RC, Fuchs RA, Wave forces on piles: a diffraction theory. *Technical Memorandum*, 1954, 69.

- [21] Maruo H, The drift of a body floating on waves. *Journal of Ship Research*, 1960: 1–10.
- [22] Mathisen J, Borrenson R, Linderberg K, In: Improved strip theory for wave induced loads on twin hull semisubmersible, *Proceedings of the First OMAE Symposium*, New Orleans, Louisiana, 1982.
- [23] Mizutani N, Iwata K, Diffraction Force on a spherical structure and wave diffraction. *Journal of Offshore and Polar Engineering*, 1993; 3(1):7-11.
- [24] Molin, B, Jamois, E. Lee CH. Newman, JN., Non linear wave with a square cylinder, In: 20th International Workshop on Water Waves and Floating Bodies, 2005.
- [25] Newman J, Low-Frequency Resonance of Moonpools, In: 18th International Workshop on Water Waves and Floating Bodies, 2003, p. 18-37.
- [26] Newman JN. The drift force and moment on ships in waves, *Journal Ship Research*, 1967,6:10-17
- [27] Newman J, Lee CH, Solution of radiation problem with exact geometry, In: 16th Workshop on Water Waves and Floating Bodies, Hiroshima, Japan, 2001, p. 93-96.
- [28] Newman J, Lee CH, Computation of wave effects using the panel method, In: *Models in Fluid-Structure Interaction*, Preprint, Editor S. Chakraborti, 2004.
- [29] Newman J, Sclavounos P, In: The computation of wave load on large offshore structure, In: 5th Int. Conf. Behaviours of Offshore Structures (Boss '88), 1988, 5.
- [30] Ogilvie TF, Second-order hydrodynamics effects on ocean platforms, In: *Proceedings International Workshop on Ship and Platform Motions*, 1983: 205-265.

- [31] Papanikolaou A, Zaraphonitis G, Investigation into the capsizing of damaged Ro-Ro passenger ships in waves. In: Proc. 7th Int. Conf. on Stability of Ships and Ocean Vehicles, 2000: 351–361.
- [32] Pinkster JA, van Oortmerssen, G. Computation of the first and second order wave forces on bodies oscillating in regular waves. In: 2nd Int. Conf. Numerical Ship Hydrodynamics 1977: 136–156.
- [33] Pinkster JA, Mean and low frequency wave drifting forces on floating structures. Ocean Engineering, 1979, 6:593-615.
- [34] Punzo V, Besio S, Pittaluga S, Trequattrini, A, Solution of Laplace Equation on non axially symmetrical volumes, IEEE Transactions on Applied Superconductivity, 2006, 16(2).
- [35] Remery GFM, van Oortmsessen G, The mean wave, wind and current forces on offshore structures and their role in the design of mooring systems, Proceedings of Offshore Technology Conference, OTC, paper no.1741, p. I-169 – I-184, 1973.
- [36] Skourup J, Fai CK, Bingham BH, Buchmann Bjarne, Loads on a 3D body due to second order waves and a current. Ocean Engineering, 2000, 27 :707-727.
- [37] Wang JP, Chung FC, Guo J, On the prediction of maneuverability of the Autonomous Underwater Vehicle, AUV-HM1. In:International Symposium on Underwater Technology, Tokyo,1988: 185-190.
- [38] Wang S, Motions of a spherical submarine in waves. Ocean Engg, 1986, 13(3): 249–271.
- [39] Wu GX, Witz JA, Ma Q, Brown DT, Analysis of wave induced drift forces acting on a submerged sphere in finite water depth. Applied Ocean Research, 1994, 16 (6): 353-361.

- [40] Zhao R, Faltinsen OM, Krokstad JR, Aanesland V, Wave-current interaction effects on large-volume structures. In: T. Moan, N. Janby and O. Faltinsen, Editors, Proc. 5th Int. Conf. Behaviours of Offshore Structures (Boss '88), 1988, 2.

APPENDIX 1

SYMBOLS

<i>Symbol</i>	<i>Meaning</i>
ϕ	Total scalar potential
\bar{F}_1	Free Surface component of Second order Drift force
\bar{F}_2	Velocity Squared component of Second order Drift force
\bar{F}_3	Translation component of Second order Drift force
\bar{F}_4	Rotation component of Second order Drift force
η_{r1}	first order wave surface elevation
η_j	local normal
\bar{F}_3	Motion component of Second order Drift force
\bar{F}_4	Rotation component of Second order Drift force
a	radius of body, axial length along major axes (in case of ellipsoid)
b	axial length along minor horizontal axes (in case of ellipsoid), Breath of the box
c	axial length along minor vertical axes (in case of ellipsoid)
d	water depth
ϕ_d	Total diffracted potential
F_{ix}	Horizontal Component of Force
F_{iy}	Vertical Component of Force
g	acceleration due to gravity
H	wave Height
ϕ_i	Total incident potential
J_n	Bessel function of first kind
k	wave number
L	length of Cylinder
p	Dynamic Pressure
R_0	Distance away from the body
R	$\sqrt{(X^2 + Y^2)}$
R'	Radius of Gyration
s_0	Depth Of Submergence
S_0	Body Surface Area
u	Horizontal water particle velocity
u_i	Velocity component along i^{th} coordinate
u_r	Radial component of velocity
u_θ	Angular, θ component of Velocity
u_μ	Angular, μ component of Velocity

v	Vertical water particle velocity
w	water particle velocity in z direction
X'	Translation Motion of Body
X	Defined in text according to geometry
Y	Defined in text according to geometry
Y_n	Bessel function of second kind
β	direction of wave propagation
ε	perturbation parameter= ka
η	Free Surface Elevation
λ_i	Axes in Ellipsoidal coordinates
ρ	Density of water
ζ	eigenvalues for the Somerfield condition
ω	angular velocity

APPENDIX 2

MATLAB CODE

Code for Ellipsoid (Fish)

```

%% Velocity Squared term for ellipsoid
%%%%%%%%%%%%%%%%%%%%%%%%%%%%%%%%%%%%%%%%%%%%%%%%%%%%%%%%%%%%%%%%%%%%%%%%%%%%%%Anupam Gupta%%%%%%%%%%%%%%%%%%%%%%%%%%%%%%%%%%%%%%%%%%%%%%%%%%%%%%%%%%%%%%%%%%%%%%%%%%%%%%

%%%%%%%%%%%%%%%%%%%%%%%%%%%%%%%%%%%%%%%%%%%%%%%%%%%%%%%%%%%%%%%%%%%%%%%%%%%%%%
                    %%% Input Variables:
%%%%%%%%%%%%%%%%%%%%%%%%%%%%%%%%%%%%%%%%%%%%%%%%%%%%%%%%%%%%%%%%%%%%%%%%%%%%%%

clc
clear all
H=200;                % Wave Height, cm

%%%%%%%%%%%%%%%%%%%%%%%%%%%%%%%%%%%%%%%%%%%%%%%%%%%%%%%%%%%%%%%%%%%%%%%%%%%%%%
                    %%% Three axes %%%%%%%%%%%%%%%%%%%%%%%%%%%%%%%%%%%%%%%%%%%%%%%%%%%%%%%%%%%%%%%%%%%%%%%%%%%%%%%
L=[100 60 30 15];    % overall length of the fish, cm

for p=1:1:4
a=0.93*L(p);          % major longitudinal axes, cm
b=0.193*L(p);         % horizontal minor axes, cm
c=0.112*L(p);         % vertical axes, cm

%%%%%%%%%%%%%%%%%%%%%%%%%%%%%%%%%%%%%%%%%%%%%%%%%%%%%%%%%%%%%%%%%%%%%%%%%%%%%%Calculations %%%%%%%%%%%%%%%%%%%%%%%%%%%%%%%%%%%%%%%%%%%%%%%%%%%%%%%%%%%%%%%%%%%%%%%%%%%%%%%
h=(a^2-b^2)^(0.5);
K=(a^2-c^2)^(0.5);
d=2*a;                % water depth
s=1.5*a;               % depth of submergence
%%%%%%%%%%%%%%%%%%%%%%%%%%%%%%%%%%%%%%%%%%%%%%%%%%%%%%%%%%%%%%%%%%%%%%%%%%%%%%

dpsi=1;
dmu=1;
dv=1;
%%%%%%%%%%%%%%%%%%%%%%%%%%%%%%%%%%%%%%%%%%%%%%%%%%%%%%%%%%%%%%%%%%%%%%%%%%%%%%
j=1;

for ka= 0.01:0.01:3;

k=ka/(H/2);
kd=k*d;

F=0;
for psi=0.1:1:a
for mu= 0.1:1:b
for v= 0.1:1:c

```



```

z=((psi^2-K^2)*(mu^2-K^2)*(K^2-v^2))^0.5/K/(h^2-K^2)^0.5;

A= (sinh(k*(s+d)))^0.5/cosh(kd)*(mu^2-K^2)*(K^2-v^2)*psi/K^2/(h^2-K^2)/z;
%% psi compenet of velocity

B= (sinh(k*(s+d)))^0.5/cosh(kd)*(psi^2-K^2)*(K^2-v^2)*mu/K^2/(h^2-K^2)/z;
%% mu compenet of velocity

C= (sinh(k*(s+d)))^0.5/cosh(kd)*(mu^2-K^2)*(K^2-psi^2)*v/K^2/(h^2-K^2)/z;
%% v compenet of velocity

D=((A^2+B^2+C^2))*v/(v^2+psi^2+mu^2)^(0.5)*psi/(psi^2+mu^2)^(0.5)*dpsi*dm
u*dv;

F=(F+D);
    end
    end
end
    F1(j,p)=abs(real(F))/a/(H/2)^2;
    FR(j,1)=F1(j,p);
    Ka(j,1)=ka;
    j=j+1;

end

plot(Ka,FR)
    title('Drift Force for Fish');
    xlabel('ka');
    ylabel('F');
    grid on;
    hold on;

end

Legend(L, 'Cod', 'Haddock', 'Harring', 'Spart');

```

Code for Sphere

```

%%%%%%%%%%%%%%%%%%%%%%%%%%%%%%%%%%%%%%%%%%%%%%%%%%%%%%%%%%%%%%%%%%%%%%%%
%%% Code for Calculation of Second order drift forces on sphere %%%
%%%%%%%%%%%%%%%%%%%%%%%%%%%%%%%%%%%%%%%%%%%%%%%%%%%%%%%%%%%%%%%%%%%%%%%%
%%%%%%%%%%%%%%%%%%%%%%%%%%%%%%%%%%%%%%%%%%%%%%%%%%%%%%%%%%%%%%%%%%%%%%%%Anupam Gupta%%%%%%%%%%%%%%%%%%%%%%%%%%%%%%%%%%%%%%%%%%%%%%%%%%%%%%%%%%%%%%%%%%%%%%%%

```

```

clc
clear all

%Input Variables
a=50; %radius
g=32.1; %gravity
H=2; %wave Height
w=1; %2*pi/T
d=200; %water depth
F=0; %initialization of Force
dx=1*pi/180; %delta theta
dy=1*pi/180; %delta mu
rho=1940; %Density
%j=1; %initialization for elements of
F1 vector

%%%%%%%%%%%%%%%%%%%%%%%%%%%%%%%%%%%%%%%%%%%%%%%%%%%%%%%%%%%%%%%%%%%%%%%%
%%%%%%%%%%%%%%%%%%%%%%%%%%%%%%%%%%%%%%%%%%%%%%%%%%%%%%%%%%%%%%%%%%%%%%%%Numerical Integration %%%%%%%%%%%%%%%%%%%%%%%%%%%%%%%%%%%%%%%%%%%%%%%%%%%%%%%%%%%%%%%%%%%%%%%%%
%%%%%%%%%%%%%%%%%%%%%%%%%%%%%%%%%%%%%%%%%%%%%%%%%%%%%%%%%%%%%%%%%%%%%%%%
for t=1:1:30
    Ka(t,1)=t/10;
end

r=[3,4,5,6];
for i=1:1:4
    d=r(i)*a; % water depth
    dth=1*pi/180; % delta theta
    s=1.5*a;
    j=1;
    for ka=0.1:0.1:3 % Loop for different values of ka
        k=ka/a; % calculation of k
        kd=k*d; % calculation of kd
        ks=ka/a*s;
        for x=1:10:180; % Integration with respect to
            theta
                for y=1:10:360; % integration with respect to mu
                    x=x*pi/180; % conversion to radians
                    y=y*pi/180; % constant value squared
                    C1=rho*g^2*H^2/16/w^2/(cosh(kd))^2; % Multiplying Factor for pressure
                    C2=cos(x)*(sin(y))^2*dx*dy; % Multiplying Factor for pressure
                    component
                    C=C1*C2;
                    X1=ka*cos(x)*sin(y);
                    Y1=ka*sin(x)*sin(y)+ks;
                    R1=(X1^2+Y1^2)^(0.5);
                    X1d=ka*cos(x)*cos(y);
                    Y1d=ka*sin(x)*cos(y);

%%%%%%%%%%%%%%%%%%%%%%%%%%%%%%%%%%%%%%%%%%%%%%%%%%%%%%%%%%%%%%%%%%%%%%%%
                    Int1t= 4*X1^2*(sinh(Y1))^2; % First term of integration
                    Int2t=(2*Y1*cosh(Y1)-sinh(Y1))^2; % Second Term of Integration

```

```

uth=C*(Int1t+Int2t);           % Total theta component
%%%%%%%%%%%%%%%%%%%%%%%%%%%%%%%%%%%%%%%%%%%%%%%%%%%%%%%%%%%%%%%%%%%%%%%%
%%%%%%%%%%%%%%%%%%%%%%%%%%%%%%%%%%%%%%%%%%%%%%%%%%%%%%%%%%%%%%%%%%%%%%%%

end                               % End of y loop
end                               % end of x loop
F=(uth);                         % Force
F1(j,i)=F;                       % final force normalized
FR(j,1)=F1(j,i);

j=j+1;                           % increament of j
end
plot(Ka,FR)
    title('Drift Force for Sphere');
    xlabel('ka');
    ylabel('F');
    grid on;
    hold on;
end

Legend(r, 'Depth/radius=3', 'Depth/radius=4', 'Depth/radius=5', 'Depth/radius
=6');

```

```

%%%%%%%%%%%%%%%%%%%%%%%%%%%%%%%%%%%%%%%%%%%%%%%%%%%%%%%%%%%%%%%%%%%%%%%%%% Velcoity Squared Term for Barge %%%%%%%%%%%%%%%%%%%%%%%%%%%%%%%%%%%%%%%%%%%%%%%%%%%%%%%%%%%%%%%%%%%%%%%%%%%
%%%%%%%%%%%%%%%%%%%%%%%%%%%%%%%%%%%%%%%%%%%%%%%%%%%%%%%%%%%%%%%%%%%%%%%%%% Anupam Gupta %%%%%%%%%%%%%%%%%%%%%%%%%%%%%%%%%%%%%%%%%%%%%%%%%%%%%%%%%%%%%%%%%%%%%%%%%%%

```

```

i=1; % initiation of loop for vector
d=15; % water depth
D=1.5; % Draft
k=0.008375; % Initial approximation of k
for w=0.01:0.01:10

    k=w^2/10/tanh(k*d); % Dispersion relationship
    F(i,1)=(sinh(2*k*d)-sinh(2*k*(d-D)))/2/cosh(2*k*d);
    W(i,1)=w; % Frequency
    i=i+1;
end
plot(W,F)

```

VITA

Anupam Gupta was born in Kota, India. He lived most of his life in India. In 2002, Anupam was accepted for the undergraduate program in civil engineering at the Institute of Technology, Banras Hindu University. He graduated with a Bachelor of Technology degree in civil engineering in 2006. He was then accepted for the graduate program at University of Illinois, Chicago in 2006. He was also employed as a teaching assistant at University of Illinois at Chicago. He studied there for one year and then transferred to Texas A&M to continue his Master of Science in civil engineering. During his stay at Texas A&M he has worked under the guidance of Prof. John M. Niedzwecki as a research assistant.

Anupam Gupta can be reached at his permanent address in India:

Anupam Gupta
4-A-11, Mahaveer Nagar Extension
Kota, Rajasthan
324009
India
Phone- +917442472178